ABSTRACT

PARAMETER OPTIMIZATION FOR CURL DISTORTION IN BUILDING PARTS USING 3-D LASER STEREOLITHOGRAPHY

by
Laurel A. Hanesian

The curl distortions in rapid prototyping using 3-D laser stereolithography occur as the top layers shrink after being drawn and attaching to the bottom layers. The amount of curl is dependent upon the how much shrinkage the layer has finished prior to adhesion. It is also dependent on how deep the cure of the top layer amounts to as it adheres into the bottom layer. This thesis investigated the effect of build parameters on the distortions associated with the H-4, diagnostic 'Letter-H' shaped test part. The same parameters were also considered in a time optimization study, using calculated, predicted results rather than empirical data. The build parameters varied for this study were layer thickness, border overcure, hatch overcure, fill cure depth, fill spacing, and hatch spacing. The material used to build the part was Ciba-Geigy Resin SL 5170 and the apparatus was a 3D Systems Corporation SLA-250 rapid prototyping system.

Experimental measurements confirm that layer thickness, hatch overcure, and hatch spacing are the three dominant parameters that affect part accuracy and account for 80 - 90 percent contribution for the distortions at the positions measured. The magnitude of distortion is dependent on the amount of resin surface area that has been cured. The smallest values of distortion occur when less than 100% of the surface has been cured. By using Taguchi orthogonal arrays an optimization study showed that smaller layer thicknesses combined with smaller hatch overcures and larger hatch spacings produced smaller distortions. Smaller layer thicknesses also produced quicker build scan times.

PARAMETER OPTIMIZATION FOR CURL DISTORTION IN BUILDING PARTS USING 3-D LASER STEREOLITHOGRAPHY

by
Laurel A. Hanesian

A Thesis
Submitted to the Faculty of
New Jersey Institute of Technology
in Partial Fulfillment of the Requirements for the Degree of
Master of Science in Mechanical Engineering

Department of Mechanical Engineering

January 1998

APPROVAL PAGE

PARAMETER OPTIMIZATION FOR CURL DISTORTION IN BUILDING PARTS USING 3-D LASER STEREOLITHOGRAPHY

Laurel A. Hanesian

12/19/97

Dr. Ming C. Leu, Thesis Advisor — Date
Professor of Mechanical Engineering, NJIT

12/19/97

Dr. Zhiming Ji, Committee Member — Date
Associate Professor of Mechanical Engineering, NJIT

12/19/97

Dr. Donald H. Sebastian, Committee Member — Date
Professor of Industrial and Manufacturing Engineering, NJIT

BIOGRAPHICAL SKETCH

Author: Laurel A. Hanesian

Degree: Master of Science in Mechanical Engineering

Date: January 1998

Date of Birth:

Place of Birth:

Undergraduate and Graduate Education:

- Master of Science in Mechanical Engineering,
  New Jersey Institute of Technology, Newark, NJ, 1998
- Bachelor of Science in Mechanical Engineering,
  New Jersey Institute of Technology, Newark, NJ, 1993

Major: Mechanical Engineering

This thesis is dedicated to
my parents, Shavasp and Laurice Hanesian
for teaching me how important it is to never give up.

ACKNOWLEDGMENT

The author would like to thank her advisor, Dr. Ming C. Leu, for providing her with the wonderful experience of learning and researching advanced manufacturing technologies. His guidance is greatly appreciated.

An expression of gratitude to Dr. Zhiming Ji and Dr. Donald H. Sebastian for reviewing this research and serving on the committee.

The assistance and cooperation provided to the author from other researchers and professionals in the field has been an enormous help. These supporters are: Dr. Zhang Wei from the Robotics and Intelligent Manufacturing Laboratory, Dr. Hyung S. Cho and research staff from KAIST, Dr. Calvin C. Chen from Lucent Technologies, and George Sladek from Sicam.

Finally thanks to Albert Yao for always being there to answer all of my questions and thanks to my uncle, Dr. Deran Hanesian for having the patience of Job.

TABLE OF CONTENTS

TABLE OF CONTENTS
(Continued)

Chapter **Page**

TABLE OF CONTENTS
(Continued)

Chapter **Page**

LIST OF TABLES

Table **Page**

LIST OF TABLES
(Continued)

Chapter **Page**

LIST OF FIGURES

CHAPTER 1

AN INTRODUCTION TO STEREOLITHOGRAPHY TECHNOLOGY

1.1 Stereolithography and its Contributions to Manufacturing

Stereolithography (SL) is a three dimensional printing of a CAD design model. This form of rapid prototyping, patented in 1986, and other solid freeform fabrication technologies have changed design and manufacturing. Having a tangible prototype in hand aids in visualizing the design because it is often difficult to read two-dimensional cross-sections or to see intricate details in a CAD image. Rapid Prototyping and Manufacturing (RP&M) also allows designers to confirm quickly the desired performance of a product ensuring quality and product reputation. This is accomplished by manufacturing a fully functional prototype once the SL prototype has been verified. Tests then can be conducted on the actual mechanical aspects of the functional prototype, such as strength, fatigue, temperature resistance, etc., to detect possible shortcomings with the design. However, with rapid prototyping, if a geometric problem is detected early on, multiple new designs can be iterated and verified in a matter of just a few days. Consequently, the optimization process of a design is not as costly or time consuming.

1.2 The Basic Process of Stereolithography Rapid Prototyping

Stereolithography technology is accomplished with the use of a photocurable resin and a focused laser beam. A CAD model is sliced into a series of horizontal cross-sections stacked one on top of another. Starting from the bottom, the laser maps out the first slice, or section. Next, the platform is displaced a given amount, known as the layer

thickness, and the laser maps out the second section. This process is repeated layer by layer until the CAD model is converted into a solid object.

1.3 Resin Polymerization

1.3.1 Resin Shrinkage

The resulting solid object is not 100% dimensionally accurate when compared to the CAD nominal values. Problems generally occur due to the tendency of the resin to shrink as it goes through its polymerization process. During the process the shear strength of the resin increases rapidly as the transition from liquid monomer to solid polymer occurs. As the strong covalent bonds form between the monomer groups a three dimensional polymer results, the distance between various monomer groups decreases, and the resulting resin becomes more dense. These changes occurring during the polymerization process as these covalent bonds are formed can affect linear shrinkage, curl, creep distortions in the green state, flatness, and swelling. Furthermore, the chemical cross-linking reaction process continues during the postcure in the postcure apparatus (PCA). The mechanical properties of the cross-linked polymer change markedly during the entire process of polymerization and the nature of the distortions that result vary. The mechanical properties of the solid polymer formed are a function of cure depth, beam diameter, hatch spacing, layer thickness, border overcure, hatch overcure, and fill spacing.

Characteristic of a non-linear, three dimensional polymer is the significant occurrence of a sharp *gel point*. This gel point occurs at a very well-defined stage in the polymerization process, the material transforms suddenly from a viscous liquid to a gel.

After the gel point, the three dimensional polymer is no longer able to melt, nor is it soluble in solvents. It is at the gel point that the physical and mechanical properties of the polymer begin to change, known as the green strength. In SL, the exposure necessary to achieve this point is the critical threshold exposure, E_c (mJ/cm^2), where the resin is in a gel state. This point is shown graphically in Figure 1.1 as the abscissa intercept of the working curve. In Figure 1.1, the two fundamental parameters, D_p, the penetration depth and E_c, the critical threshold exposure are both necessary to define the polymer photospeed and, hence, the actual laser scan velocity. Additional discussion regarding photospeed and scan velocity can be found in Section 2.4.

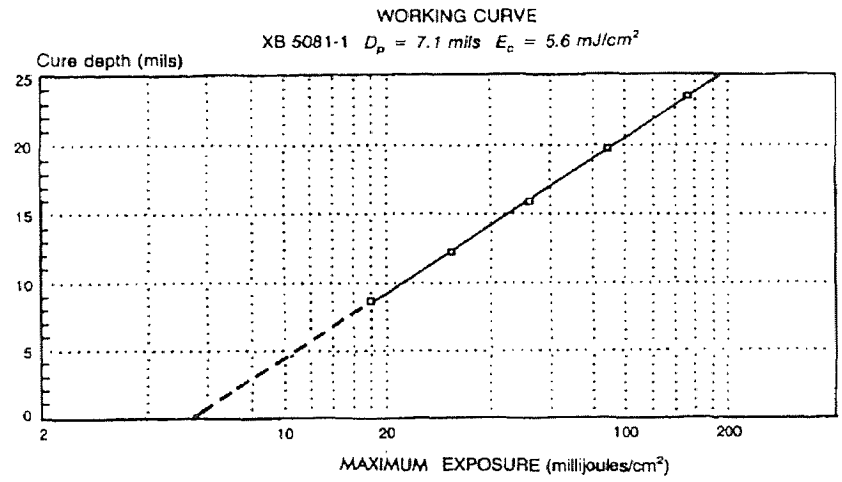

Figure 1.1 The Working Curve for Ciba-Giegy resin XB 5081-1.
Source: Jacobs, Paul F. et al. Rapid Prototyping and Manufacturing: Fundamentals of Stereolithography (New York: McGraw-Hill, 1992) p. 89

1.3.2 The Working Curve Equation

The Working Curve is a semilog plot of cure depth, C_d (mils), versus maximum exposure, E_{max} (mJ/cm^2), obtained from the working curve equation:

$$C_d = D_p ln(E_{max}/E_c)$$

where D_p = Penetration Depth (mils).

"This equation is absolutely fundamental to SL. [It] states in mathematical form, the following five basic points:

1. The cure depth is proportional to the natural logarithm of the maximum exposure on the centerline of the scanned laser beam.
2. A semilog plot of C_d vs. E_{max} should be a straight line. This plot is known as the working curve for a given resin.
3. The slope of the "working curve" is precisely D_p, the penetration depth of that resin, at the laser wavelength.
4. The intercept of the working curve, specifically the value for the exposure at which the cure depth is zero, is simply E_c , the critical exposure of that resin, at the laser wavelength.
5. Since D_p and E_c are purely resin parameters, then both the slope and the intercept of the working curve are independent of laser power."

(Jacobs 1992, p. 88)

Although the resin begins to gel at E_c, it has no mechanical strength. Green strength is the term used to describe mechanical properties of a photocured part, i.e. hardness, strain, modulus, etc. The green strength has to be sufficient enough for the part

to be able to hold its shape throughout the build and postcure processes. It also has to be great enough to limit distortions. The principal parameter necessary to increase green strength is energy, specifically the energy in excess over E_c.

1.4 Curl Distortion and Related Improvements

1.4.1 Curl Distortion Defined

A common distortion that occurs during the build process is curl distortion. This happens because stereolithography is a layer additive process, therefore the top layers shrink after being drawn and attaching to the bottom layers. The curl manifests itself mostly in flat, horizontal slabs and unsupported cantilever beams.

1.4.2 The WEAVE Build Method

The first great improvement on accuracy due to curl distortion occurred in 1991 with the introduction of the WEAVE build pattern. During the development of WEAVE, experimental observations showed that curl distortion was directly related to the amount of shrinkage that occurred after attaching to the previous layer, as stated before. With this in mind, the WEAVE method intentionally draws the first layer of the internal hatch vectors with a cure depth less than the layer thickness. Figure 1.2 shows an isometric view of a single cured line and a cross-sectional view of four cured lines. These hatch

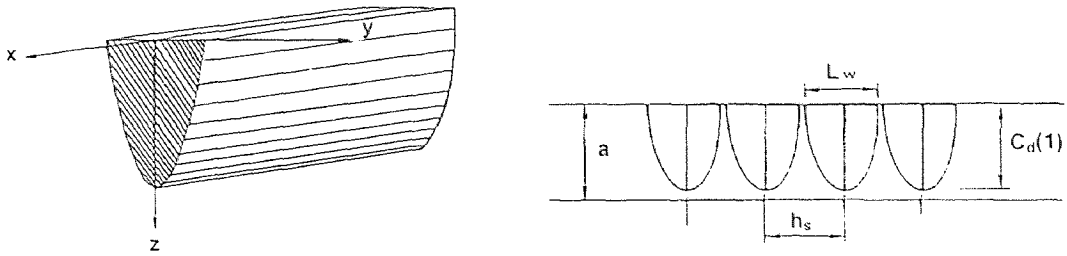

Figure 1.2 Views of cured lines, where a = layer thickness, L_w = line width, h_s = hatch spacing, and $C_d(1)$ = the cure depth of 1 laser pass.
Source: Jacobs, Paul F. et al. Rapid Prototyping and Manufacturing: Fundamentals of Stereolithography (New York: McGraw-Hill, 1992) p. 87, p. 206.

vectors are free to shrink without causing distortion because they are not yet attached to the former layer. Next, another set of hatch vectors are drawn orthogonally to the prior hatch vectors, shown in Figure 1.3. The points of intersection create an overcure bullet

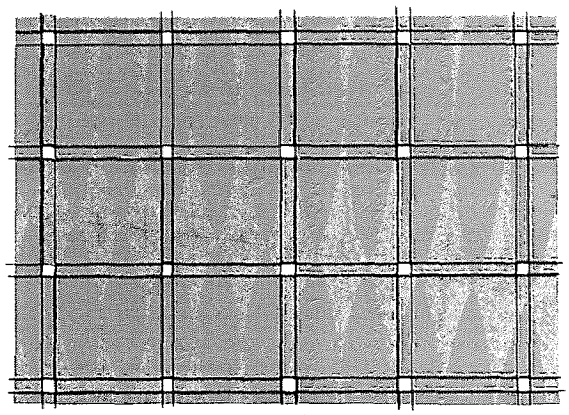

Figure 1.3 Cross pattern of x and y hatch vectors. The large square boxes indicated points where the vectors have intersected (double cure) thus causing overcure bullets. The small, white boxes are points where the laser has not cured any material, and the long, skinny, rectangular areas are of single pass cure.
Source: Jacobs, Paul F. et al. Rapid Prototyping and Manufacturing: Fundamentals of Stereolithography (New York: McGraw-Hill, 1992) p. 207.

that bonds the layers together without contributing to excessive overcure or undercure. This balances distortions due to the increase of shrinkage with excessive overcure and the delamination due to undercure.

1.4.3 The STAR-WEAVE Build Method

Further improvements came from the development of the STAR-WEAVE build method. The name is derived from **ST**-staggered hatch, **A**-alternate sequencing, and **R**-retracted hatch. The concept of staggered hatch is to offset each successive layer of vectors half of the previous hatch spacing, similar to the way a brick wall is layered. This reduces stress concentrations. Alternate sequencing allows for a difference in the order of the hatch vectors. For example, for layer 1 the y-hatch vectors were drawn first, followed by the x-hatch vectors. For layer 2 the order is reversed and the x-hatch vectors are drawn first with the y-hatch vectors following. This prevents any possibility of a pattern causing distortions in a specified area. Finally, the retracted hatch reduces shrinkage distortions at the borders. This is accomplished by alternating which side the hatch vector attaches to the border. The borders of each layer are drawn first and the hatch is used to fill them in. As an example of retracted hatch, the first x-hatch vector attaches to the right side border and scans across the layer until just short of the left side border. The second x-hatch vector displaces some defined value for hatch spacing distance along the y-axis and attaches now to the left side border scanning across the layer until it falls just short of the right side border. The third x-hatch vector then moves further up the y-axis and attaches to the right border but falls short of the left. This pattern repeats itself alternating scanning direction in a zigzag type motion until all of the bordered area has been filled

for a given layer. The process is also true for hatches scanned along the y-axis and displacing along the x-axis. Previously, in other build methods the hatch vectors were attached to both borders. This caused greater distortions due to shrinkage forces and action-reaction principles of force pulling in each direction on the border.

1.4.4 Epoxy Resins

The next major improvement came in 1993 with the introduction of the epoxy resins. The properties of these polymers provided for stronger parts with less shrinkage than parts made with acrylate resins. In general, for epoxy resins, there is minimal volume change on reaction because the number and type of chemical bonds formed in polymerization are essentially identical to those before reaction. Acrylates, on the other hand, convert a double bond to a single bond in polymerization causing changes in bond length.

1.4.5 The ACES Build Method

The acronym ACES stands for **A**ccurate, **C**lear, **E**poxy, **S**olid parts. These parts are accomplished by ensuring near complete cure during the build process. If cure is close to 100% during the build portion of the process, post-cure distortions are essentially eliminated. Also, the ACES build method uniformly polymerizes the epoxy resin by using two consecutive passes of UV radiation, all of this is done prior to adhering to the previous layer. As discussed with earlier build methods, this reduces any possibility for internal stress build up by having the previous layers begin shrinking while the next layers are being drawn and attached.

CHAPTER 2

LITERATURE SURVEY

2.1 The Forces Which Cause Curl Distortions are Still Relevant Today

Regardless of the improvements made toward rectifying curl distortions, the deformations of an unsupported cantilever are still of relevant significance today. For most practical applications, a part built with the latest resins and build methods, provided it had adequate supports, will be extremely accurate and unaffected by curl distortions. The relevancy is apparent when the supports are removed and the internal stresses, which are built up from the same forces that produced the curl distortions in the build process, produce a latent curl, or creep distortion.

2.1.1 The H-4 Diagnostic Test Part

3D Systems Corporation developed the H-4 test part shown in Figure 2.1 to study the distortion significance regardless of the apparatus or resin used. This is accomplished by using one point of data as a reference point and comparing it to the other sets of data. This concept is discussed in further detail in Chapter 4, Materials and Experimental Methods. The dotted lines in the figure represent an exaggerated example of a distorted part. There are three modes of distortion associated with the H-4 test part. They are in-vat distortion, post-support removal distortion, and post-cure distortion.

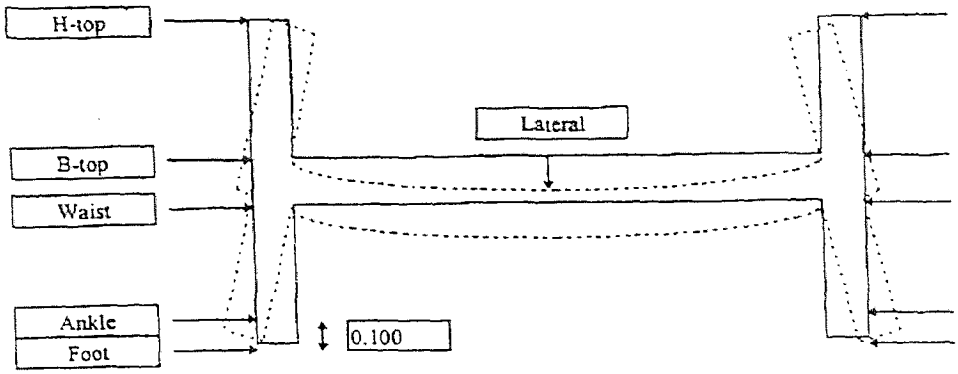

Figure 2.1 The H-4 Diagnostic Test Part.
Source: Pang, Thomas H., Michelle D. Guertin, and Hop D. Nguyen. "Accuracy of Stereolithography Parts: Mechanism and Modes of Distortion for a 'Letter-H' Diagnostic Part" *Proceedings of North American Stereolithography User Group Conference and Annual Meeting* 1994.

2.2 The Distortions of the H-4 Diagnostic Test Part

2.2.1 The In-Vat Distortion

The in-vat distortion occurs during the actual build process. The distortion at the "waist" is due directly to curl. As the first layer of the long horizontal section of the 'H' is drawn, its shrinkage causes the legs to deflect inward. As more layers are cured and the previous layers gain in strength, the shrinkage forces decrease. This phenomenon was first recognized in early experiments regarding curl distortions in cantilevers. The first layer actually drawn deforms in a downward direction. The more common upward curl distortion occurs when the subsequent layers are added. This is due to the shrinkage forces of the layers; these forces introduce a bending moment. However, as more layers are added, the strength of the thicker section is able to resist the distortion.

Some early predictions of how to reduce curl distortion are listed below:

"1. Use high exposure and slow scan speed such that polymerization is essentially complete under the laser spot.

2. Use a resin with a faster rate of polymerization.

3. Decrease laser power to decrease scan speed for a given exposure.

4. Use a low-shrinkage resin.

5. Increase layer thickness to increase strength."

(Jacobs 1992, p. 43)

Hunziker and Leyden, authors of the chapter cited above, discussed experimental results based on these predictions. A summary of relevant material follows.

Figure 2.2 shows the graphical results of curl factor vs. overcure for three different resin types; GA-EA, GM-EA, and GA-EM, where, GA - Glyicidyl Acrylate, GM - Glycidyl Methacrylate, EA - Ethoxy Acrylate, and EM - Ethoxy Methacrylate. For the experiment used to collect the data shown in Figure 2.2, layer thickness was set at 10 mils. By definition cure depth = layer thickness + overcure. Theoretically, without overcure, layers would not be bonded together, but just touching, therefore free to shrink without causing stress in previous layers. However, a connection is required between layers in order to hold the part together. Increasing the exposure until polymerization is complete only increases overcure and promotes greater curl distortions.

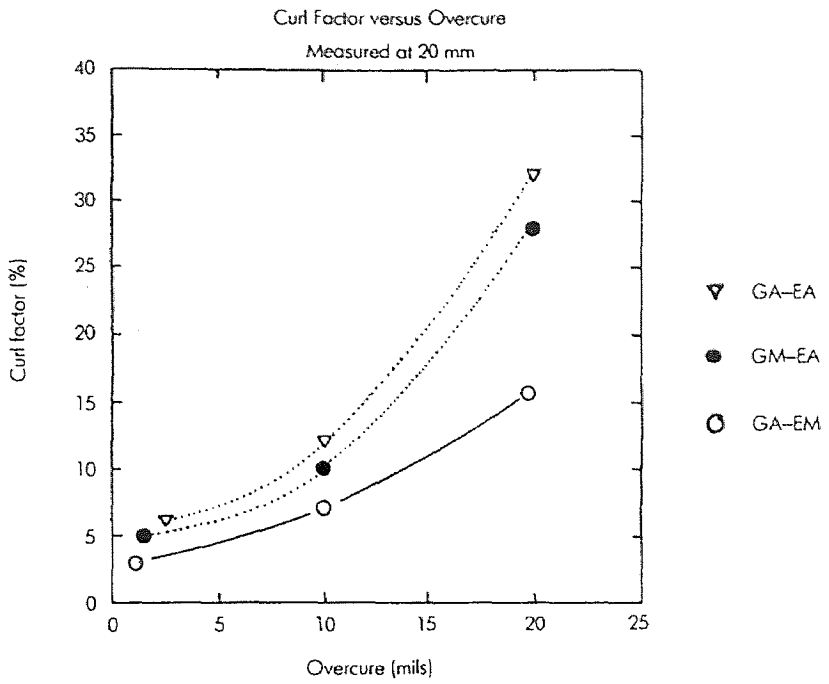

Figure 2.2 Curl Factor versus Overcure for three different resins.
Source: Jacobs, Paul F. et al. Rapid Prototyping and Manufacturing: Fundamentals of Stereolithography (New York: McGraw-Hill, 1992) p. 45

Experiments using an SLA-250 with Cibatool XB 5081-1 and varying laser power from 2 to 9 mW did not show a significant increase in curl. Similar results were concluded using the SLA-500. The reason for these results was that the shrinkage which causes curl, lags behind drawing speed even at the lowest laser power.

Total volumetric shrinkage of a resin clearly is related to curl distortion. However, it is not a direct relation as one would assume. A study between GA-EA and GA-EM showed that although their shrinkage factors were essentially the same, the curl distortions could be quite different. The acrylate based system yielded a much greater curl than the methacrylate system. Similar results have been produced using more recent epoxy resins such as Ciba-Geigy SL 5170 and SL 5180.

2.2.2 The Post-Support Removal Distortion

The post-support removal distortion in the H-test part is also caused by curl. This distortion is due to the allowance of the legs to splay outward once the part is removed from the platform. Because of the relaxation of internal stresses built up from the effects of curl, it is referred to as a latent curl, or creep distortion. These stresses move the H-Top arms inward and the Ankle/Foot legs outward.

SL parts should be postcured immediately after building to yield the best results. However, for a variety of reasons this is not always possible. A part may finish its building process during off business hours and left sitting on its supports in the green state until the next business day. In addition, parts may take detailed cleanup work or data may need to be collected, delaying the time before postcure takes place. It has been noted with the earlier acrylate resins that green parts left for extended periods of time without postcuring would show greater dimensional errors. The errors were known to increase when the parts remained in the green state.

Green creep distortion (GCD) is plotted against time, shown in Figure 2.3, for three Ciba-Geigy acrylate resins, SL 5081-1, SL 5143, and SL 5249; all were built using the STAR-WEAVE method. Also plotted are the Ciba-Geigy epoxy resins, SL 5170 and SL 5180. These were built using the QuickCast build method. It was noted that data collected for the solid ACES style had similar results. These results indicate a much

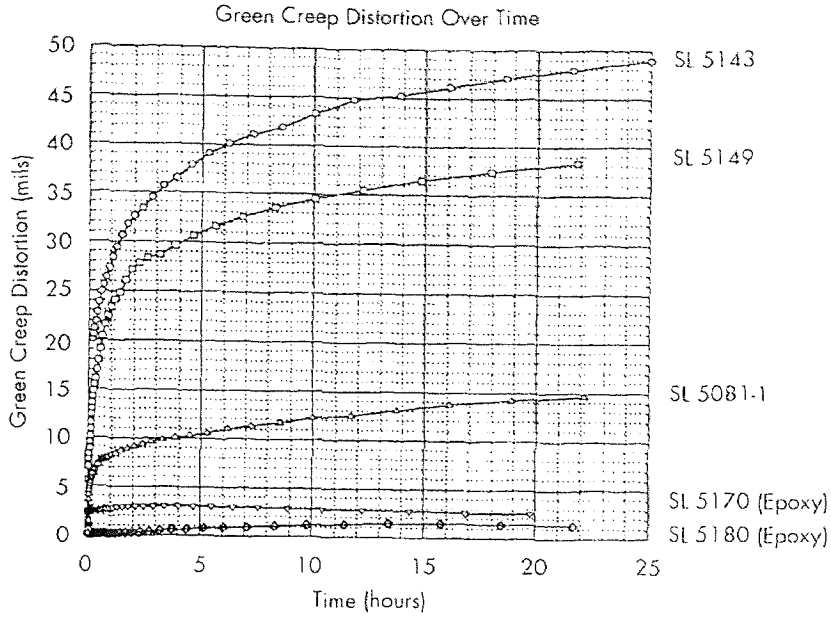

Figure 2.3 Green Creep Distortion versus Time.
Source: Jacobs, Paul F. et al. Stereolithography and Other RP&M Technologies: from Rapid Prototyping to Rapid Tooling (New York: ASME Press, 1996) p. 44.

lower green creep distortion rate for the epoxy resin compared to the acrylate. Also it points out that the GCD rate for the epoxy resins after the initial distortion is a negligible variation regardless of time.

2.2.3 The Post-cure Distortion

Due to any remaining uncured material after the build process within the SLA, distortions may occur during the final postcure stage in the UV oven. However, the method used to postcure the H-4 test part causes negligible distortions along the five measurements taken H-Top, B-Top, Waist, Ankle, and Foot. The method is presented in Chapter 4. "The expected postcure distortion is mostly in the plane of the H-4 part when postcured in this manner. The distortions in the plane of the H-4 part are not considered for this diagnostic. The inhomogeneous part of the postcure distortion relative to the dimension

at B-Top, is expected to be small enough for this geometry such that it can be neglected for this test." (Pang, Guertin, and Nguyen, 1995, p. 174)

2.3 Influence of Build Parameters on Curl Distortion

A similar study was performed at the University of Delaware changing the build parameters layer thickness, hatch overcure, hatch spacing, fill overcure, and writing styles. The writing styles varied between Tri-hatch and Star-WEAVE. The resin used was DuPont SOMOS 3110, an urethane acrylate based resin. The model used was the Twin Cantilever diagnostic test part. This model is in the shape of a 'T' having unsupported cantilevers on either side of its base.

A summary of relevant significant conclusions from this study were:

- The results of the experimental study show that these five parameters are quite significant in explaining the curl behavior.
- From the data analysis results it is observed that of the two writing styles investigated, the tri-hatch style yields better results in terms of lower curl distortions as well as a better modeling of the curl behavior.
- Layer thickness is a very significant factor influencing the curl behavior. Data analysis at the various layer thicknesses yields some interesting results. With tri-hatch writing style it is observed that lower curl distortions can be obtained using 5 mil and 10 mil layer thicknesses. However, the curl behavior at 7.4 mil layer thickness is markedly different. The magnitudes of the distortions were very high.

> The substantially higher levels of curl distortion observed suggests a non-linear behavior of curl with layer thickness.
>
> (Jayanthi 1995, p. 82)

At first glance, the second conclusion regarding tri-hatch yielding better results than WEAVE seems contradictory to the improvement summary provided in Chapter 1. However, this result actually supports the already published data for cantilever curl distortion. It is defined as the curl elevation per unit length along the cantilever and is expressed as a percentage (Jacobs 1992, p. 256). A comparison of various acrylate based resins show that twin cantilevers built using the WEAVE method had cantilever curl distortions of 2 - 4 % higher than tri-hatch methods. This displayed that curl distortion was dependent on resin type and build method. It also showed that resins with lower viscosities yielded higher curls.

Advances in polymers provided SLA users with epoxy resins. Using the appropriate build method with the appropriate epoxy resin provides for lower curl distortions. The H-4 diagnostic test part shows significant improvements using an epoxy resin, SL 5170, with the ACES build method over an urethane-acrylate resin, SL5149, with the STAR-WEAVE build method.

2.4 Build Time

Along with dimensional accuracy, the amount of time it takes to build a prototype is of great concern to industry. If a stereolithographic part were to take too long to make, the concepts behind rapid prototypes would be lost. It is therefore important to know prior to the build how long the prototype will take to make. Dr. Calvin Chen of Lucent

Technologies has developed a build time estimator to predict the total scan time and recoat time of a stereolithography model.

This is done essentially by using information stored in the slice files of an SLA-250 machine. Specifically the ".v" and ".r" files. The ".v" file is a geometric file consisting of all the vectors necessary to determine the direction of the triangle face determined by the tessellation of the CAD image as put into .STL format. The .STL format breaks the CAD image into a series of triangles, whose vertices are given in x, y, and z coordinates. The ".r" file holds all of the information the SLA needs to run the appropriate build parameters for each layer of the part. Dr. Chen's program combines the information from both of these files to calculate the theoretical velocity:

$$V_s = \sqrt{(2/\pi)}\,\frac{P_L}{W_o E_c}\quad e^{(-C_d/D_p)}$$

Where P_L = laser power (mW),
E_c = critical exposure (mJ/cm^2)
V_s = scan velocity (cm/sec)
C_d = cure depth (mils)
D_p = penetration depth (mils)
W_o = beam radius (cm)

The easiest controlled parameter in the above equation would be the cure depth. It shows that increasing the cure depth for any given part decreases its scan velocity exponentially. The actual velocity is always slower than the theoretical velocity by a factor of 0.68 - 0.75. Therefore the scan velocity calculated is the theoretical velocity multiplied by a velocity factor (0.685) which was determined through trial and error. This program provided for very accurate results, "maximum error is about ½ hours even for a 36 hour job." (Chen and Sullivan, 1996)

The above equation represents the scan velocity which is a function of the scan time representing only part of the total build time. The other portion of the total build time is due to the time necessary to properly recoat the layer surface area prior to the next laser scan. The recoat time is dependent on parameters, as an example, postdip delay - the time the elevator remains in its dip position underneath the surface of the resin and z-wait - the number of seconds the elevator pauses before beginning the next laser scan.

Time is therefore controlled mostly by the defined cure depth and surface area of the part; larger surface areas need increased postdip delays.

CHAPTER 3

OBJECTIVE

The objective of this study is to determine how variations of build parameters affect curl distortions in SLA parts. A Letter-H diagnostic test part is used to quantify the interactions. The parameters are layer thickness, border overcure, hatch overcure, fill cure depth, fill spacing, and hatch spacing. A study will be conducted to determine the combinations of build parameters that provide for minimal distortion. In addition, the study will determine if an optimal set of parameters that minimizes distortion compromises build time. A build time estimation program will be used to understand the relationship between parameter variation and build time, and whether or not users have to comprise accuracy for build time and vice versa.

CHAPTER 4

EXPERIMENTAL METHODS

4.1 Material

The material used in this study was Ciba-Geigy SL 5170. Its properties are:

E_c = 13.5 mJ/cm^2

D_p = 4.8 mils

4.2 Apparatus

4.2.1 The Stereolithography Apparatus

3D Systems Corporation's SLA-250 rapid prototyping system uses a helium-cadmium laser to cure the resin. Below is a schematic of the elements of a stereolithographic system. To obtain the extremely focused laser spot necessary to make precise cured lines,

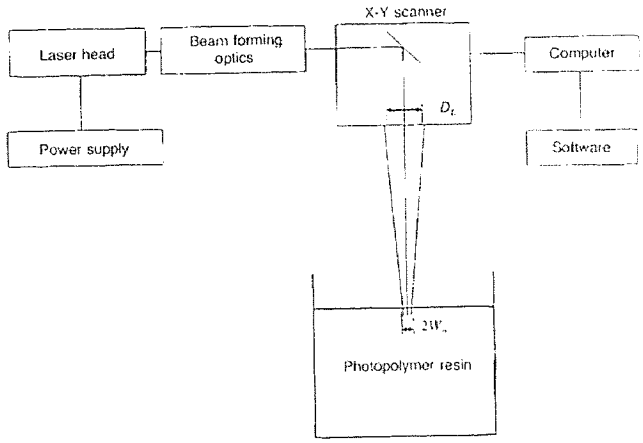

Figure 4.1 Schematic of a stereolithographic system.
Source: Jacobs, Paul F. et al. Rapid Prototyping and Manufacturing: Fundamentals of Stereolithography (New York: McGraw-Hill, 1992) p. 61.

the HeCd laser is shot into a beam-expanding telescope where beam scanning mirrors focus the emission some distance, L, at the surface of the resin.

4.2.2 The Postcure Apparatus

After the initial build process the part is postcured in the postcure apparatus (PCA). This is an oven with a continuous ultra violet lamp inside.

4.3 The H-4 Diagnostic Test Part

4.3.1 What Makes the H-4 Test Part a Good Diagnostic Part?

The H-4 test part is a diagnostic part developed to make resin comparisons. It was chosen as the part for this study because "it is also less dependent on the calibration status of particular RP&M machines, and is excellent for the purpose of generating simple but meaningful accuracy information, which can be used to further understand the mechanism and the modes of distortion in RP&M materials." (Pang, Guertin, and Nguyen, 1995, p. 170)

4.3.2 The Relevant Dimensions Involved

Five dimensions are identified for this part; they are H-Top, B-Top, Waist, Ankle/Foot, and Lateral, shown in Figure 2.1. The nature of the distortions associated with this part keeps the dimension of B-Top relatively close to the nominal CAD value. To keep the data collected independent of the apparatus used, the B-Top value is used as an internal reference rather than the nominal CAD value of four inches. Distortion is therefore the

difference of each dimension with respect to the B-Top dimension. In other words, data collected from four separate SLA-250 machines has no effect on the results of the resin tested.

4.3.3 Three Modes of Distortion

There are three modes of distortion related to this part. They are in-vat distortion, post-support removal distortion, and postcure distortion. Of most importance to this study are the in-vat distortions due to curl and the post-support removal distortions due to creep. Postcure distortions have been assumed to cause equal shrinkage for the dimensions mentioned before. Due to the nature of the postcure process, described in detail in Section 4.4, the distortions are anticipated to lie in the H-4 plane therefore not affecting the five critical dimensions.

4.4 Procedure

4.4.1 Results of a Previous Comparison Study

As mentioned before, the H-4 test part was developed to make comparisons between various resins. In the paper, "Accuracy of Stereolithography Parts: Mechanism and Modes of Distortion for a 'Letter-H' Diagnostic Part", SL 5170 was compared to SL 5180 and SL5149. In this comparison test, only the default parameters of the SLA were used and the results for SL 5170 were given in Table 4.1. It is the intention of this study

Table 4.1 Distortion (mils) vs. B-Top as reference

	Green State	Postcured State
dH-Top	-2.4	-2.9
dB-Top	0.0	0.0
d-Lateral	1.8	1.4
dWaist	-11.6	-11.6
dAnkle	2.8	2.4
dFoot		

Source: Pang, Thomas H., Michelle D. Guertin, and Hop D. Nguyen. "Accuracy of Stereolithography Parts: Mechanism and Modes of Distortion for a 'Letter-H' Diagnostic Part" *Proceedings of North American Stereolithography User Group Conference and Annual Meeting* 1994.

to analyze the effects of parameter variation. By using Taguchi orthogonal arrays an optimum set of parameters will be determined to provide the least distortion, while understanding the effect of each parameter on accuracy. An L25 array allows up to six factors each with five levels. The chosen factors are listed below:

1. Layer Thickness
2. Border Overcure
3. Hatch Overcure
4. Fill Cure Depth (Up Facing - UF / Down Facing - DF)
5. Fill Spacing
6. Hatch Spacing

Each factor listed is a user defined variable within the 3D Systems Maestro Workstation Software.

Layer Thickness

The layer thickness is the individual thickness of each layer created during the build process. The acceptable range of values for this parameter is 0.004 - 0.020 in..

Border Overcure

The border overcure is the depth of cure beyond the layer thickness. The allowable range has a lower limit of, the negative value for the inputted layer thickness, and an upper limit of 0.020 in.. This means that for each build of a part, the border overcure can never be less than the negative value of layer thickness. For example, if the layer thickness is defined as 0.006 in, then the minimum allowable border overcure value is -0.006 in. Border cure depth is defined as:

$$\text{Border Cure Depth} = \text{Layer Thickness} + \text{Border Overcure}$$

Hatch Overcure

Hatch overcure has the same definition as border overcure, but it pertains to the hatch vectors. The allowable range has a lower limit of, the negative value for the inputted layer thickness, and an upper limit of 0.020 in.. Hatch cure depth is defined as:

$$\text{Hatch Cure Depth} = \text{Layer Thickness} + \text{Hatch Overcure}$$

Fill Cure Depth

This is the actual cure depth value of the fill vectors.

Fill Spacing

This is the spacing between fill vectors, measured from the center of the fill vector to the center of the next adjacent vector. The allowable range is 0.003 - 0.010 in.

Hatch Spacing

Hatch spacing has the same definition as fill spacing but in regards to hatch vectors. The allowable range is 0.005 - 0.010 in.

Table A.1 and Table B.1 found on pages 50 and 55, respectively, show both of the orthogonal arrays used to collect data for this study. All of the test models were built varying the parameters listed above in accordance with the variation combination provided by the array. The sweep mechanism has been turned off to ensure that the previously drawn layer does not get swept off such as in building small delicate parts. Z-wait, the time the platform pauses underneath the resin prior to repositioning itself for the next layer, has been increased to 45 seconds, allowing for a complete recoat of the resin prior to the next draw scan.

After the build is complete the parts are measured at the H-Top, B-Top, Waist, Ankle, and Foot dimensions using calipers. The lateral dimension can not be measured directly using calipers, but can be readily calculated. This dimension is a function of the H-Top and B-Top dimensions. In this study, the lateral dimension was not calculated and only the 5 dimensions measured along the side of the 'H' were recorded. The postcure for each part should be uniform. The total postcure is for one hour on one side only. After postcure, the parts are measured again at the same dimensions. Each measurement recorded is the average of three separate measurements taken at each dimension.

CHAPTER 5

RESULTS AND DISCUSSIONS

5.1 Original Data

The original input parameters and related outputs are listed in Appendix A. This set of 25 experiments followed the parameter combination patterns outlined for an L25 Taguchi Orthogonal Array, which is described in the next section. Only 20 out of the 25 experiments gave measurable output data. This destroyed the orthogonal nature of the array, making any statistical analysis extremely difficult. As a result, this set of data was scrapped and a new set was developed to run the second group of experiments. However, some useful observations were made from the first set of data and this information was used to formulate a new approach and set of values for the second group of experiments.

Probably the most significant observation was the large amount of variation between measurements made using standard calipers. One of the reasons for choosing the "letter-H" diagnostic part was the simplicity involved in measuring it with only calipers. This decision was based upon the statement,

> "The in-vat waist "tucking" distortion, latent lateral curl distortion that occurs following the support removal, and the splaying out of the arms and the legs are easily measured using standard calipers. A CMM or high precision specialty equipment is not necessary for this diagnostic, unless a more precise work is required. Linear green build shrinkage and postcure shrinkage can be easily calculated from the diagnostic part. Lateral curl on the horizontal section, which was not previously accessible for measurement with a caliper, can now be

> accurately calculated from the distance between the H-4 arms measured using calipers." (Pang, Guertin, and Nguyen 1995, p. 179)

This statement proved not to be true for this study. It was difficult to place the calipers in the exact intended position for each measurement. It was also difficult to ensure the calipers were flush, at a right angle to the sides of the H-part, and not skewed which would alter caliper readings. Most importantly, the vice motion of the caliper would cause further deflection of the legs of the H-part, giving unreliable data. As a result any further measurements were made on a CMM (Coordinate Measurement Machine). This machine has a delicate diamond tip, therefore any measurements taken were from completed post-cured parts and not in the green state.

Another lesson learned from the original set of data was the importance of hatch overcure to the build process. As an oversight, a value of -0.005 in. was chosen for one of the variations for hatch overcure. However, when layer thickness is set at 0.004 in. this value for hatch overcure is out of range by definition, as stated in Chapter Four. This combination occurred in trial #1 and produced a hollow structured part because the resulting internal hatch cure depth for this particular set of parameters is -0.001 in., which is impossible.

The reasons for the remaining four failures are unknown. Trial #10 did not build any structure at all. Trials #19, #21, and #22 all had extremely rough surface finish due to extra uncured material floating in the vat during the build process. For an unknown reason, during these builds a thin film of cured material was observed floating on the surface of the resin. Once the build process was complete and the platform was elevated completely out of the liquid resin, the floating material draped itself over the H-parts that

happened to be under it at the time. It is assumed that the particular parameter combinations for trials #19, #21, or #22 did not have anything to do with their rough surface finishes. Another build under the exact same parameter combinations would have to be performed in order to verify whether or not the phenomenon of floating material is repeatable. One observation made between the first 25 sets of experiments and the second set is the difference in laser power. The second set did not use the same input for parameter variation, therefore, a true comparison can not be made. For the second build, the laser power was running at almost twice the power of the first build. Perhaps, when the laser power is running low the focus of the laser beam is not as accurate causing the thin film of cured material to float upon the top of the resin surface. Another assumption would question how layer delamination may affect the amount of unattached cured material floating in the vat. However, based on observations this event is highly unlikely. Of the two sets that had extra cured material (trials 16 - 20 and trials 21 - 25), all five H-parts in each set were solid without any sign of delamination on the part itself. Generally when delamination occurs, the actual dislocation of layers is apparent. However, with these parts, this was not the case.

5.2 Statistical Methods

5.2.1 Taguchi Orthogonal Arrays

A variety of build parameters were studied in order to determine relationships between these parameters with part accuracy and/or build time. By the traditional method of collecting data, a number of experiments would be conducted where one parameter is varied while the others remain constant. This process is reiterated until all parameters

have been studied on an individual level. Considering this study has a total of six parameters at five different levels, the total number of experiments needed to perform the classical method is 5^6 or 15,625 experiments; it is quite obvious that this approach would be costly and time consuming. Therefore a decision to use the L25 Taguchi orthogonal array, shown in Table 5.1, was made. Taguchi arrays are based upon the concepts behind fractional factorial experiments. The orthogonality of the matrix indicates for any two columns, any possible combination of factor levels will occur an equal number of times. For the L25 array there are 5 x 5 possible factor level arrangements, (1,1), (1,2), (1,3), (1,4), (1,5), (2,1), (2,2), (2,3), (2,4), and so on.

Table 5.1 The L25 array

Exp. No.	1	2	3	4	5	6
1	1	1	1	1	1	1
2	1	2	2	2	2	2
3	1	3	3	3	3	3
4	1	4	4	4	4	4
5	1	5	5	5	5	5
6	2	1	2	3	4	5
7	2	2	3	4	5	1
8	2	3	4	5	1	2
9	2	4	5	1	2	3
10	2	5	1	2	3	4
11	3	1	3	5	2	4
12	3	2	4	1	3	5
13	3	3	5	2	4	1
14	3	4	1	3	5	2
15	3	5	2	4	1	3
16	4	1	4	2	5	3
17	4	2	5	3	1	4
18	4	3	1	4	2	5
19	4	4	2	5	3	1
20	4	5	3	1	4	2
21	5	1	5	4	3	2
22	5	2	1	5	4	3
23	5	3	2	1	5	4
24	5	4	3	2	1	5
25	5	5	4	3	2	1

Source: Phadke, Madhav S. Quality Engineering Using Robust Design (Englewood Cliffs, NJ: Prentice Hall, 1989) p. 292.

5.3 The Second Set of Data

5.3.1 Effects of Factor Levels

"The effect of a factor level is defined as the deviation it causes from the overall mean." (Phadke 1989, p. 45) These effects are determined by averaging the outputs caused by each effect. As an example, the results for dH-Top at a layer thickness of 0.006 in. are 0.005 in., 0.004 in., 0.004 in., 0.003 in., 0.003 in. and their average is 0.0038 in.. Once all of the effects are calculated for each parameter an optimization can be determined and used as a prediction to lessen variations caused by parameter combinations. For this

study the goal is to decrease the amount of deflection from nominal, along the length of the letter 'H'. The optimum values chosen are therefore the minimum values for each parameter set. Tables B.3 - B.7 found on pages 57 - 61 indicate these results.

To begin optimizing the distortion caused at H-Top, two parameter sets have been predicted, as shown in Table 5.2. Two sets of predicted optimums occurred for dH-Top

Table 5.2 dH-Top optimal parameter sets. All dimensions are in inches.

dH-Top		
Layer Thickness	0.004	0.004
Border Overcure	0.007	0.007
Hatch Overcure	-0.004	-0.004
Fill Cure Depth (Up/Down Facing)	0.009/0.013	0.009/0.013
Fill Spacing	0.006	0.006
Hatch Spacing	0.006	0.010

because the effects of hatch spacing at 0.006 in. and 0.010 in. both produced a minimum distortion value of 0.0058 in.. It is interesting to note that the parameter set in the 2nd column matches the parameter combination for trial #10, which is the only trial that failed to build a successful part. The resulting H-part for trial #10 was void of hatch, similar to trial #1 of the original data collected. This is due to the equation:

$$\text{Hatch Cure Depth} = \text{Layer Thickness} + \text{Hatch Overcure}$$

In trial #10 this equation yields $0 = 0.004 + (-0.004)$, therefore causing no hatch to occur.

although extra precaution was taken to ensure the parameters were in the recommended limits. As defined in the 3D Systems Maestro Workstation User Guide, "Hatch Overcure - This field shows values for Hatch vectors. These overcure values may be changed. The allowable range is [the negative value of] layer thickness to 0.0200 in." (User Guide, p. 50).

The optimum parameter sets for the distortion at the remaining locations, Waist, Ankle, and Foot due to minimum factor effects are shown in Tables 5.3 and 5.4. Clearly,

Table 5.3 dWaist optimal parameter sets. All dimensions are in inches.

dWaist				
Layer Thickness	0.004	0.004	0.006	0.006
Border Overcure	0.011	0.011	0.011	0.011
Hatch Overcure	-0.003	-0.004	-0.003	-0.004
Fill Cure Depth (Up/Down Facing)	0.003/0.007	0.003/0.007	0.003/0.007	0.003/0.007
Fill Spacing	0.006	0.006	0.006	0.006
Hatch Spacing	0.010	0.010	0.010	0.010

Table 5.4 dAnkle and dFoot optimal parameter sets. All dimensions are in inches.

dAnkle		dFoot	
Layer Thickness	0.004	**Layer Thickness**	0.004
Border Overcure	0.013	**Border Overcure**	0.013
Hatch Overcure	-0.004	**Hatch Overcure**	-0.004
Fill Cure Depth (Up/Down Facing)	0.005/0.009	**Fill Cure Depth (Up/Down Facing)**	0.005/0.009
Fill Spacing	0.006	**Fill Spacing**	0.006
Hatch Spacing	0.010	**Hatch Spacing**	0.010

there are numerous combinations to choose from. In order to predict a more accurate set of data we must understand which parameters contribute the most to the distortions for all locations along the H-part.

5.3.2 Analysis of Variance (ANOVA)

To gain a better understanding of which parameters are contributing most to the distortion, an analysis of variance was performed. To provide an example, the data of Waist will be used. Full tables of results for each location of measure can be found in Tables B.8 - B.15 on pages 62 - 65. The equations are:

$$\text{Grand total sum of squares} = \sum_{i=1}^{25} \text{dwaist}_i^2$$

$$= 0.005686 \text{ in}^2$$

$$\text{Sum of squares due to mean} = (\#\text{ of experiments}) \times \text{overall mean}^2$$

$$= 0.00467856 \text{ in}^2$$

$$\text{Total sum of squares} = \sum_{i=1}^{25} (\text{dwaist}_i - \text{overall mean})^2$$

$$= 0.00100744 \text{ in}^2$$

As a check, the total sum of squares is also equal to the difference between the grand total sum of squares and the sum of squares due to mean.

$$(0.005686 - 0.00467856 = 0.00100744)$$

The sum of squares due to a certain factor was determined as follows:

SS of parameter layer thickness (LT) =

5*(the effect of LT @ 0.006 in. - overall mean)^2 +

5*(the effect of LT @ 0.004 in. - overall mean)^2 +

5*(the effect of LT @ 0.008 in. - overall mean)^2 +

5*(the effect of LT @ 0.012 in. - overall mean)^2 +

5*(the effect of LT @ 0.010 in. - overall mean)^2

=0.00049024 in^2

To determine the percent contribution of each parameter, divide the sum of squares of the parameter by the total sum of squares and multiply by 100.

0.00049024/0.00100744*(100) = 48.66 %

Therefore the percent contribution layer thickness has on the distortion at the Waist is 48.66%. The following table summarizes the results for each location and parameter studied. From this table it is apparent that layer thickness is the dominant parameter

Table 5.5 The percent contributions at each measurement location for each parameter.

	dH-Top	dWaist	dAnkle	dFoot
Layer Thickness	58.62%	48.66%	49.06%	48.15%
Border Overcure	6.75 %	7.01%	3.89%	8.00%
Hatch Overcure	14.72%	15.63%	20.92%	20.04%
Fill Cure Depth	7.81 %	4.79%	1.49%	4.08%
Fill Spacing	6.17 %	2.01%	2.73%	0.92%
Hatch Spacing	5.94%	21.90%	21.91%	18.80%

affecting distortions. Hatch overcure is clearly also an important parameter. The majority of measurements are affected by hatch spacing, with the exception of H-Top. H-Top's results imply that hatch spacing is relatively insignificant to its distortion. The next greatest contributor after hatch overcure, for H-Top, would be fill cure depth. It is assumed that this result occurs because fill vectors are drawn on top and bottom facing surfaces, with H-Top being measured along a top facing surface. However, this factor does not play a significant role for the measurement at Foot because this bottom facing surface is connected to the supports offering protection against distortion. The distortion at the foot does not really occur until after the build process is complete and the H-part is removed from its supports. The relaxation of built-up internal stresses causes the feet and ankles of the H to splay outward.

Another possibility for the deviation from the layer thickness, hatch overcure, and hatch spacing pattern in the H-Top results may be due to the unacceptable data gathered for trial #10. Based on results from similar studies and the majority of measurements that fit the pattern, layer thickness, hatch overcure, and hatch spacing will be considered to be dominant regardless of location along the side of the 'H'. The lower four contributing parameters for H-Top are all in the same order of magnitude, implying a relatively insignificant effect toward distortion compared to the two dominant parameters, layer thickness and hatch overcure. Therefore focusing on optimizing hatch spacing rather than fill cure depth will have little effect on the distortions at H-Top.

5.3.3 Trial #10 Compensation

It is obvious that the measurements collected for trial #10 are grossly inaccurate. To compensate for this, the same statistical analysis was performed using a set of data made from the average of the other 24 collected outputs in a substitution for trial #10. It is assumed that this approach would produce more useful information rather than the actual values. Interestingly, the analysis produced quite different results than expected. The predicted parameter sets to minimize distortion are shown in Table 5.6. The contribution

Table 5.6 Estimation for trial #10 (average 24 experiments) - Optimal parameter sets All dimensions are in inches.

	dH-Top	dWaist	dAnkle	or	dFoot
Layer Thickness	0.006	0.006	0.006	0.006	0.006
Border Overcure	0.013	0.011	0.013	0.013	0.013
Hatch Overcure	-0.004	-0.003	-0.004	-0.004	-0.004
Fill Cure Depth	0.003/0.007	0.003/0.007	0.005/0.009	0.005/0.009	0.005/0.009
Fill Spacing	0.010	0.004	0.04	0.008	0.008
Hatch Spacing	0.006	0.008	0.010	0.010	0.010

percentages per factor are given in Table 5.7. Comparing these values to the actual

Table 5.7 Estimation for trial #10 (average 24 experiments) -The percent contributions at each measurement location for each parameter.

	dH-Top	dWaist	dAnkle	dFoot
Layer Thickness	63.36%	45.91%	47.33%	43.35%
Border Overcure	9.12%	12.68%	14.00%	17.76%
Hatch Overcure	4.58%	13.02%	10.89%	11.84%
Fill Cure Depth	3.44%	8.61%	12.37%	14.28%
Fill Spacing	8.06%	1.64%	2.99%	2.01%
Hatch Spacing	11.43%	18.15%	12.41%	10.76%

collected values previously listed, many differences and similarities are readily apparent. From the results of this analysis the conclusion that hatch overcure and hatch spacing as dominant parameters can not be corroborated with the actual collected data results. Also, the distribution of percent contribution tends to be similar in magnitude between the other parameters. As an example, in the data for

dH-Top, border overcure, fill spacing, and hatch spacing range from 8.06% to 11.43% implying they all have roughly the same amount of significance. At a glance the information provided in this table does not agree with previous conclusions of this study or similar works. However, one similarity of particular interest is the magnitude of the percent contribution obtained by layer thickness. Based on the large magnitude of layer thickness contribution another assumption was made to further simulate more reasonable values for trial #10. This time the same analysis was performed where the outputs for trial #10 were the average of the other 4 data sets collected at layer thickness of 0.004 in. (trials #6,7,8, and 9). The results are provided in Tables 5.8 and 5.9. This set of data is in

Table 5.8 Estimation for trial #10 (average LT 0.004) - Optimal parameter sets
All dimensions are in inches.

	dH-Top	dWaist	dAnkle	or	dFoot
Layer Thickness	0.006	0.006	0.004	0.004	0.004
Border Overcure	0.013	0.011	0.013	0.013	0.013
Hatch Overcure	-0.004	-0.003	-0.004	-0.004	-0.004
Fill Cure Depth	0.003/0.007	0.003/0.007	0.005/0.009	0.005/0.009	0.005/0.009
Fill Spacing	0.010	0.004	0.004	0.008	0.008
Hatch Spacing	0.006	0.010	0.010	0.010	0.010

Table 5.9 Estimation for trial #10 (average LT 0.004) -The percent contributions at each measurement location for each parameter.

	dH-Top	dWaist	dAnkle	dFoot
Layer Thickness	67.78%	47.77%	50.56%	46.58%
Border Overcure	7.22%	9.51%	10.54%	14.25%
Hatch Overcure	6.81%	14.41%	13.59%	14.58%
Fill Cure Depth	3.33%	6.41%	8.51%	10.41%
Fill Spacing	6.19%	1.66%	1.72%	0.804%
Hatch Spacing	8.65%	20.23%	15.08%	13.38%

closer agreement with the layer thickness, hatch overcure, and hatch spacing dominance conclusion. Border overcure in these results contributes a much greater amount. In dH-Top it is actually the third most significant parameter. Again, the only true consistency between all three analyses, actual data, average of 24 trials, and the average of the four other trials set at layer thickness of 0.004 in., is the dominance of layer thickness ranging with contributions from 43.35% to 67.78%.

It is difficult to make any solid conclusions from this study using the statistical concepts previously described. Having one set of data missing or invalid, destroys the orthogonality of the matrix and provides for a very difficult analysis. Other noise factors also alter the results of data distributed in an orthogonal array. As an example, it can be shown in the slice files for the 25 parts that the five of the parts were built using tri-hatch instead of the STAR-Weave hatching. This is attributed to operator error and has to be viewed as another factor variance, however, it doesn't follow the pattern of the prescribed L25 array, as shown in Table 5.1. Other noise factors are laser power, time between build finish and post-cure, time between post-cure end and measurement, etc..

5.3.4 Verification of Layer Thickness, Hatch Overcure, and Hatch Spacing as Dominant Parameters

In order to verify the dominance of layer thickness, hatch overcure, and hatch spacing, another approach was considered without relying on the statistics used in orthogonal arrays. A pattern can be shown between the three parameters in simple mathematical relationships. Recall that the cross-section of a cured line is a parabola, the point at the vertex is considered the cure depth and the distance where the function intersects the top of the resin represents the linewidth. The following equations show that linewidth is a function of both parameters, overcure and layer thickness:

Cure Depth = Layer Thickness + Overcure

Linewidth = $B\sqrt{(Cd / 2Dp)}$

Percentage of resin cured at top of surface = (Linewidth/Hatch Spacing) *(100)

where B = laser spot diameter, approximately 9 mils for the SLA laser.
C_d = Cure Depth, mils
D_p = Penetration Depth, approximately 4.8 mils for SL 5170
(Jacobs, et al. 1992, p. 92, p. 205)

The hatch spacing of the vectors is the distance from center line to center line of each hatch vector. If the linewidth exceeds the value for hatch spacing, an overlap of hatch vectors will occur. This may lead to excessive curing which has been noted to cause greater curl distortions. This phenomenon can be seen in Figures 5.1 through 5.4 which show comparisons between the distortions and the percentage of cured resin. Note the values of distortion are all absolute values for these graphs. To show the amount of distortion in relation to the amount of surface cure, only magnitude was considered and not the direction the leg of the 'H' was deflecting. Again it is apparent that all of the

measurement locations fit a pattern with layer thickness, hatch overcure, and hatch spacing except dH-Top. In these graphs the collected data for the second run of experiments was used and trial #10 was discarded as inaccurate. Consistently the smallest values of distortion occur when the percentage of surface cure is less than 100%. Greater than 100% provides the situation of excessive cure as described above. Note how distortion increases and decreases in the same pattern as percentage of cure.

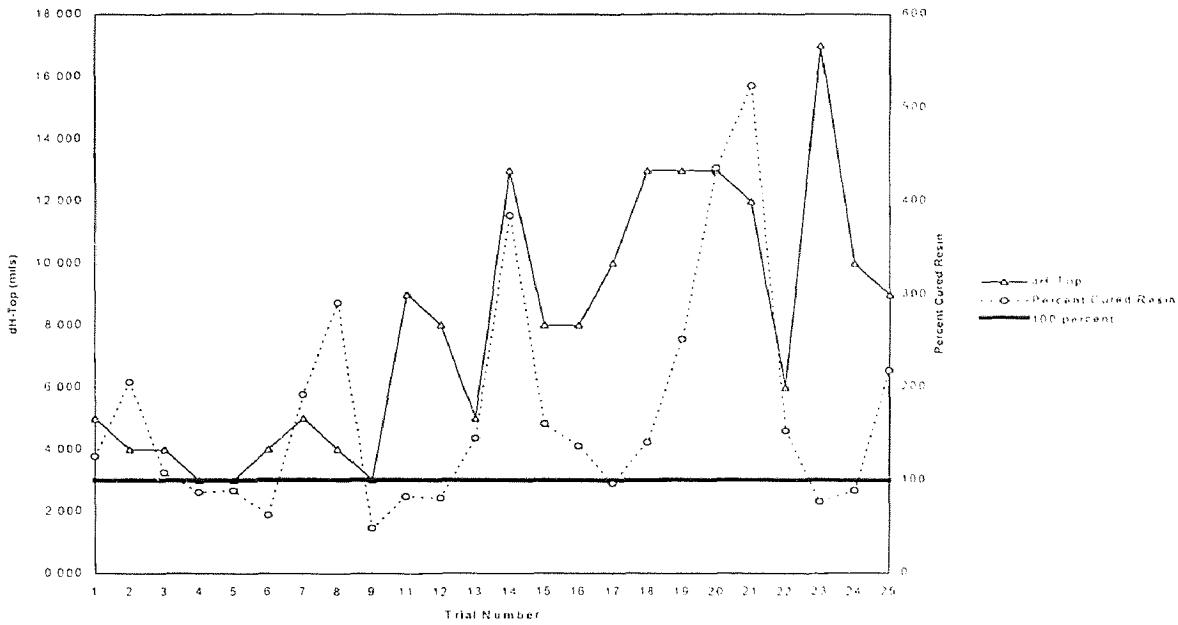

Figure 5.1 dH-Top and Percent Cured Surface Resin for 24 Trials

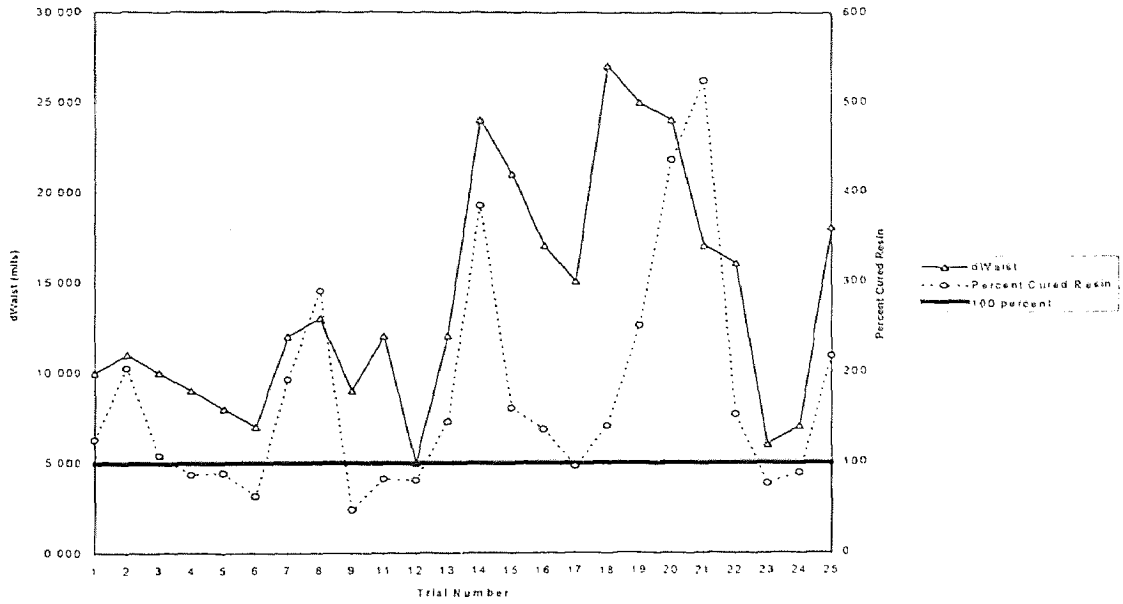

Figure 5.2 dWaist and Percent Cured Surface Resin for 24 Trials

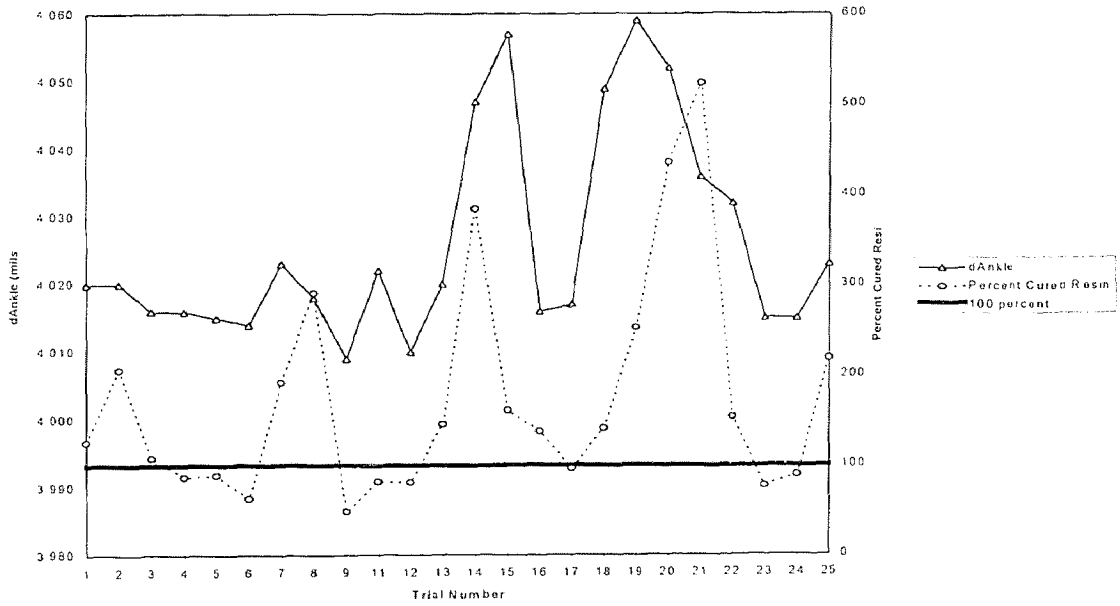

Figure 5.3 dAnkle and Percent Cured Surface Resin for 24 Trials

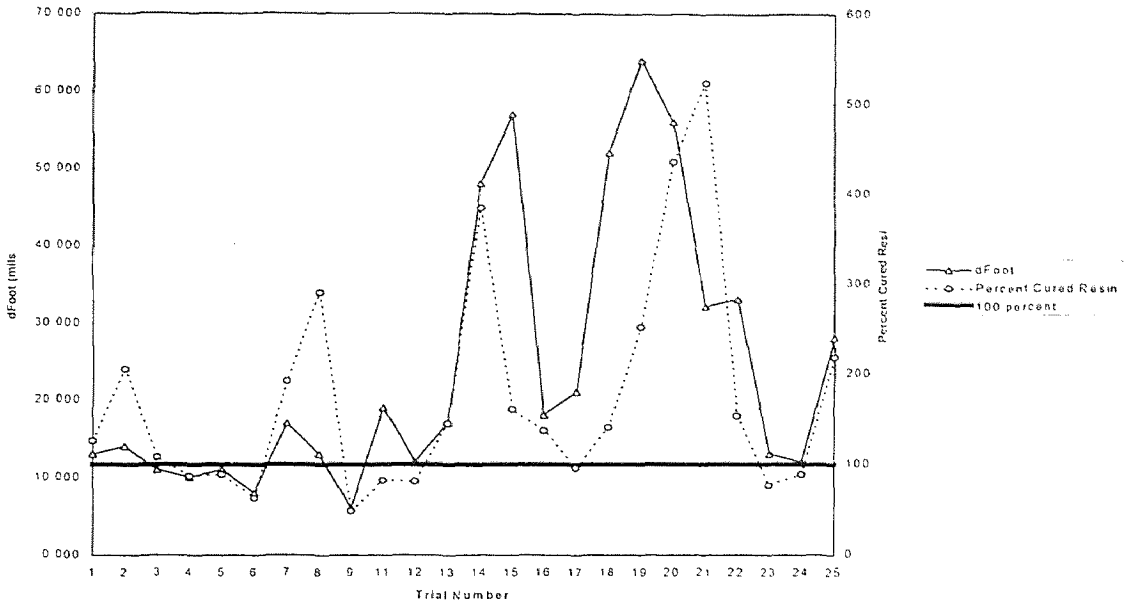

Figure 5.4 dFoot and Percent of Cured Surface Resin for 24 Trials

To verify the repeatability of this pattern a set of graphs were composed using the original data from the first set of 25 experiments collected during the initial stage of this study. The L25 orthogonal array set up for these 25 parts and their results are shown in Figures A.1 - A.4 on pages 52 - 53. The data collected for these initial 25 parts were discarded due to 5 trials that produced unmeasurable parts, as previously described in detail, destroying the orthogonal property of the array. Again the statistics would be very difficult to perform on the data collected of the 20 remaining trials. However, using the mathematical relationships described each trial can be viewed and judged independently. The patterns essentially remain the same; a couple of points may not act as expected. The data collected for these 25 trials are not considered reliable data. Many uncontrolled noise factors became issues with the initial set of experiments. Factors such as, personal

mistakes due to first time use, low laser power, and incorrect measuring devices. Due to the unreliable nature of this first set of data a firm conclusion of repeatability can not be stated, however, it appears that a strong correlation between distortion to percentage of surface cure exists.

5.4 Time Optimization

Now that it has been concluded that layer thickness, hatch spacing, and hatch overcure are the dominant factors driving the distortions along the legs of the H-part, the questions are: which factors control build time and will minimizing distortion increase time? To determine these values, a build time estimation program, developed by Dr. Chen of Lucent Technologies, was used. This program uses the sliced files, particularly the ".r" and ".v" files to estimate the build time. There were a total of five build files for this study consisting of five H-parts each. In order to use statistical analysis, as described before, a time output for each trial would be needed. Running the build time estimation program against the actual sliced files would provide a total of only five time outputs. To get the desired output the ".r" file was manually edited using the workstation's text editor, creating 25 separate files simulating actual sliced files created using the 3D Systems Maestro Workstation software. Table 5.10 provides a summary of this analysis. Actual data collected can be found in Tables C.1 - C.4 on pages 67 - 69. From this table

Table 5.10 Time optimal parameter set and percent contributions.

Time		
Layer Thickness	0.004 in.	43.54%
Border Overcure	0.005 in.	43.68%
Hatch Overcure	0.000 in.	6.00%
Fill Cure Depth	0.007/0.011 in.	5.08%
Fill Spacing	0.006 in.	0.88%
Hatch Spacing	0.002 in.	0.81%

we see that the dominating parameters are layer thickness and border overcure, both essentially equal in contribution at roughly 44%. Another factor that is apparent is the rather small value for layer thickness. At first it could be assumed that larger layer thicknesses would build faster parts because less layers are needed. However, this is not the case.

> "The laser scan velocity decreases exponentially with increased cure depth. Depending upon laser power, resin photosensitivity, and the area being scanned, the quickest layers to build are generally between 0.005 in. and 0.010 in. thick. Layers 0.005 in. thick scan in less time than those of 0.010 in. layers but require more than twice the recoating time. ...If scanning time consumes the vast majority of the build period, it may be advisable to use a smaller layer thickness to speed up the build." (Jacobs, et al. 1992, p. 177)

For this particular study the recoat time ran approximately 10 hours for each H-part built, and the scan times ranged from 0.064 to 1.349 hours. The scan times, in this case, are negligible to the overall build time.

Logically it is obvious that the internal hatch would require the most total scan time in the build process. If this is true, why didn't hatch overcure have a more significant percent contribution? Based on the prior statements made regarding the relationship between laser scan velocity and cure depth, it is assumed that the small values inputted for hatch overcure produce very fast laser scan velocities. However, the statistical analysis does not take into account the number of passes the laser is required to make in order to create the internal hatch structure. This approach leads to the conclusion that the internal hatch is not significant to overall time. Therefore the author does not agree with the conclusion that hatch is insignificant to overall time, and is hesitant to recommend using this method of optimizing build time vs. parameter input.

CHAPTER 6

CONCLUSIONS AND RECOMMENDATIONS

6.1 Conclusions

- Layer thickness, hatch overcure, and hatch spacing are the driving build parameters that control deviations in the H-4 test part.
- Smaller layer thicknesses and hatch overcures, while larger values for hatch spacing provide predicted optimal settings.
- Hatch cure depth improves distortion as it approaches zero.
- Layer thickness is a controlling factor to the total scan time.
- Smaller layer thicknesses provide for fastest scan times of the diagnostic H-4 test part. However, this will not be true for any part with a larger resin surface area.
- Many other existing "noise" factors such as laser power or resin type could affect accuracy.
    - While the SLA was running at a lower laser power, extra uncured material was observed in the vat.
    - Approximately 10 H-parts were built using a Dupont Somos resin and the initial parameter combinations set up in the original data array when the set of experiments was aborted due to poor quality of the H-parts built.
    - It was observed that layer delamination seemed to occur at the base of the H-part and in other various locations throughout the part.

- On good, solid H-parts built, distortions were smaller than those observed with Ciba-Geigy SL5170.

6.2 Recommendations

- Postcure distortions were not measured in this study based on theories drawn during the design and testing of the H-4 diagnostic part. This decision was made also due to inconvenient times when the parts were finished and the delicate nature of the diamond tip of the CMM. The statistical optimization given by the orthogonal array indicates a larger hatch spacing will provide for smaller distortions. However larger values for hatch spacing may also leave a greater percentage of uncured material within the interior of the part. This may show significant differences between measurements taken in the green state versus post cure readings. Another study to determine the trade off between hatch spacing and postcure distortion would be useful in focusing in on optimal parameters.
- Hatch cure depth cannot ever reach zero or the part will be void of internal structure. However, the optimization predictions gathered in this study show best results when the hatch overcure is closer to the negative value of layer thickness (i.e. layer thickness = 0.004 and hatch overcure = -0.004). Further studies to indicate how close to zero the cure depth can approach and how this limit effects accuracy would be interesting.
- To more accurately study parameter effect on build time, empirical data should be collected. The trade-off between length of scan time and length of recoat time is

based on scanned surface area of the layer. It is recommended to understand build time fully, an experiment with varying surface areas should be considered.

- Laser power is not an easily user adjusted parameter, however, it would be interesting to compare data at varying laser powers. How does power affect the focus of the beam; is the extra cured material a result of low beam diffusion from the low laser power?
- To avoid user bias and extra deflection caused by the vice motion of standard calipers, alternate measuring devices should be used. A CMM was the measurement device of choice for this study.
- Smaller, more manageable orthogonal arrays should be used to gain further knowledge on the three dominant parameters.
- Similar data could be collected to determine if these parameters affect other materials and test shapes in a similar way.

APPENDIX A

THE ORIGINAL DATA

The following pages include the original inputs of the L25 array used for the initial set of experiments and data collected in this study, a table of the outputs, as measured by CMM, and a series of charts showing a pattern comparison between distortion and percentage of cured surface resin. The charts only show 20 of the 25 trials due to 5 trials producing non-measurable parts.

Table A.1 Orthogonal Array for the First Set of Experiments

Trial	Layer Thickness	Border Overcure	Hatch Overcure	Fill Cure Depth (UF/DF) Up Facing/Down Facing	Fill Spacing	Hatch Spacing
1	0.004	0.000	-0.005	0.000/0.004	0.003	0.004
2	0.004	0.005	-0.003	0.002/0.006	0.004	0.005
3	0.004	0.007	-0.002	0.005/0.009	0.005	0.010
4	0.004	0.010	0.000	0.008/0.012	0.008	0.015
5	0.004	0.015	0.005	0.011/0.015	0.010	0.020
6	0.006	0.005	-0.002	0.000/0.004	0.008	0.020
7	0.006	0.007	0.000	0.002/0.006	0.010	0.004
8	0.006	0.010	0.005	0.005/0.009	0.003	0.005
9	0.006	0.015	-0.005	0.008/0.012	0.004	0.010
10	0.006	0.000	-0.003	0.011/0.015	0.005	0.015
11	0.008	0.007	0.005	0.000/0.004	0.004	0.015
12	0.008	0.010	-0.005	0.002/0.006	0.005	0.020
13	0.008	0.015	-0.003	0.005/0.009	0.008	0.004
14	0.008	0.000	-0.002	0.008/0.012	0.010	0.005
15	0.008	0.005	0.000	0.011/0.015	0.003	0.010
16	0.010	0.010	-0.003	0.000/0.004	0.010	0.010
17	0.010	0.015	-0.002	0.002/0.006	0.003	0.015
18	0.010	0.000	0.000	0.005/0.009	0.004	0.020
19	0.010	0.005	0.005	0.008/0.012	0.005	0.004
20	0.010	0.007	-0.005	0.011/0.015	0.008	0.005
21	0.015	0.015	0.000	0.000/0.004	0.005	0.005
22	0.015	0.000	0.005	0.002/0.006	0.008	0.010
23	0.015	0.005	-0.005	0.005/0.009	0.010	0.015
24	0.015	0.007	-0.003	0.008/0.012	0.003	0.020
25	0.015	0.010	-0.002	0.011/0.015	0.004	0.004

Table A.2 Output Data for the First Set of Experiments

TRIAL	H-TOP	dH-TOP	B-TOP	dB-TOP	WAIST	dWAIST	ANKLE	dANKLE	FOOT	dFOOT
1	0.000	0.000	0.000	0.000	0.000	0.000	0.000	0.000	0.000	0.000
2	4.004	0.005	4.008	0.000	3.998	0.010	4.018	0.009	4.024	0.016
3	3.995	0.015	4.010	0.000	4.003	0.007	4.025	0.015	4.029	0.020
4	3.997	0.006	4.004	0.000	3.995	0.009	4.014	0.010	4.016	0.013
5	4.000	0.007	4.008	0.000	4.004	0.004	4.022	0.015	4.024	0.016
6	4.004	0.001	4.005	0.000	4.007	0.002	4.003	0.003	4.006	0.001
7	3.997	0.009	4.006	0.000	3.998	0.009	4.018	0.012	4.023	0.017
8	3.992	0.019	4.011	0.000	3.996	0.015	4.019	0.008	4.032	0.021
9	3.999	0.008	4.006	0.000	4.002	0.005	4.008	0.001	4.010	0.004
10	0.000	0.000	0.000	0.000	0.000	0.000	0.000	0.000	0.000	0.000
11	3.994	0.012	4.006	0.000	3.993	0.013	4.017	0.012	4.026	0.020
12	4.003	0.005	4.007	0.000	4.006	0.002	4.007	0.000	4.009	0.002
13	3.991	0.009	4.000	0.000	3.989	0.011	4.016	0.016	4.019	0.019
14	3.998	0.010	4.009	0.000	3.996	0.013	4.022	0.013	4.035	0.026
15	4.001	0.007	4.007	0.000	3.998	0.010	4.013	0.006	4.017	0.009
16	4.003	0.004	4.007	0.000	3.999	0.008	4.013	0.006	4.020	0.013
17	4.009	0.002	4.007	0.000	4.002	0.005	4.017	0.010	4.020	0.013
18	4.005	0.002	4.007	0.000	4.014	0.007	4.022	0.014	4.031	0.023
19	0.000	0.000	0.000	0.000	0.000	0.000	0.000	0.000	0.000	0.000
20	4.000	0.010	4.010	0.000	3.998	0.011	4.017	0.008	4.019	0.009
21	0.000	0.000	0.000	0.000	0.000	0.000	0.000	0.000	0.000	0.000
22	0.000	0.000	0.000	0.000	0.000	0.000	0.000	0.000	0.000	0.000
23	3.999	0.010	4.009	0.000	4.002	0.008	4.017	0.008	4.018	0.009
24	3.991	0.009	3.999	0.000	3.991	0.008	4.005	0.005	4.013	0.014
25	3.974	0.034	4.008	0.000	3.999	0.008	4.043	0.035	4.051	0.043

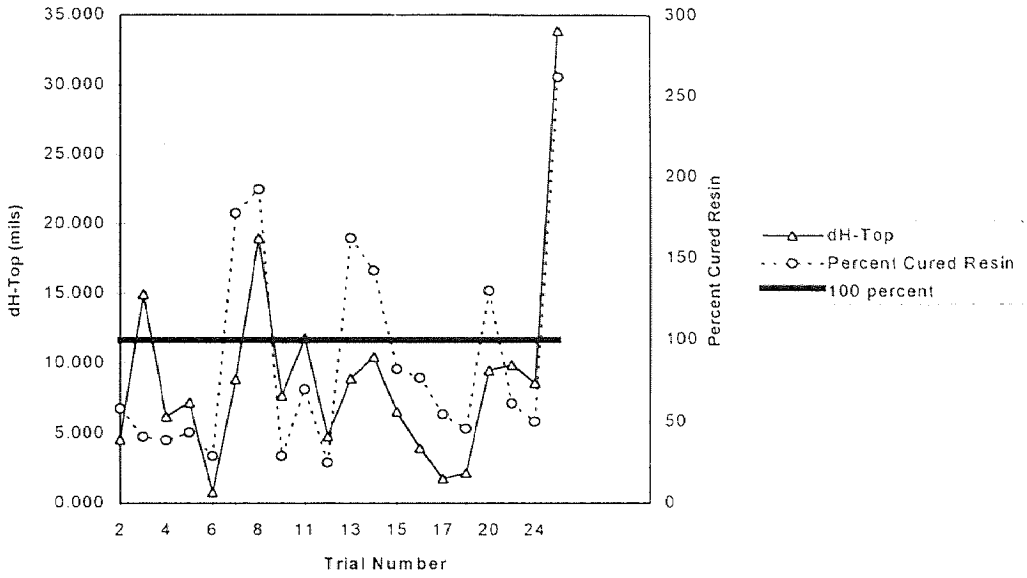

Figure A.1 dH-Top and Percent Cured Surface Resin for 20 Trials (First Set of Experiments)

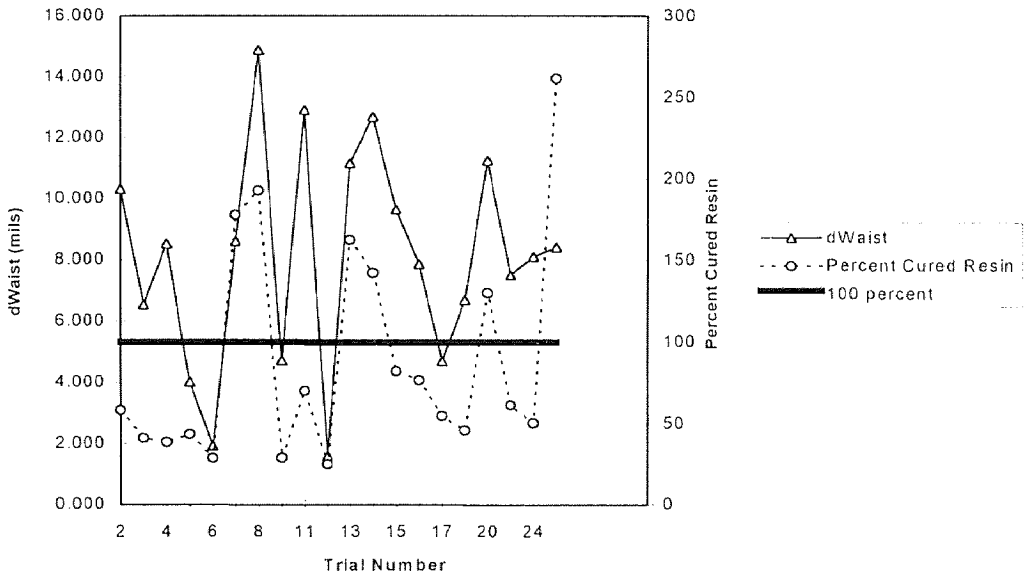

Figure A.2 dWaist and Percent Cured Surface Resin for 20 Trials (First Set of Experiments)

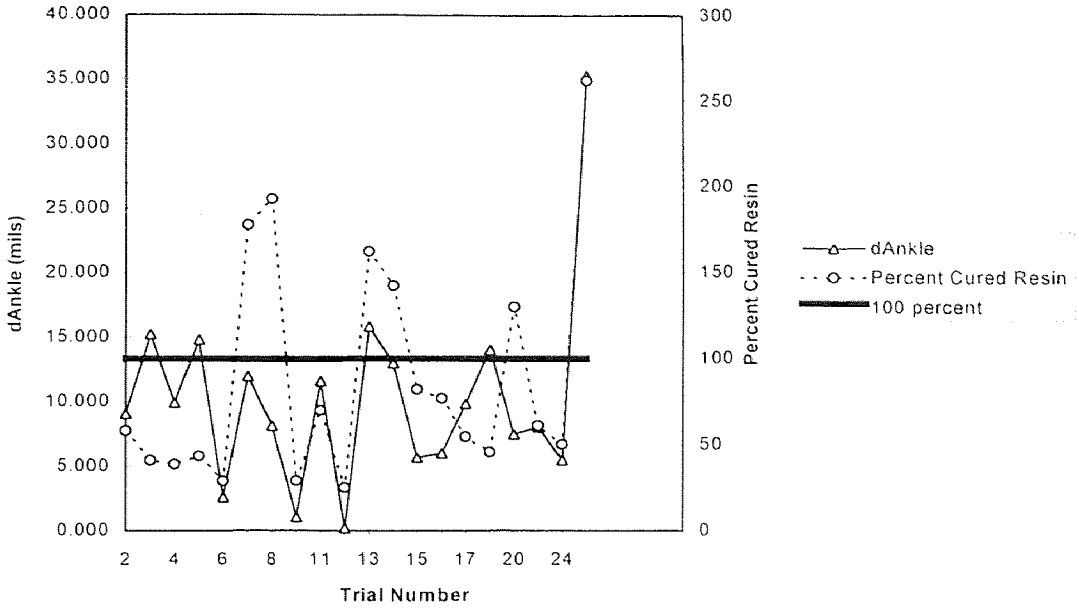

Figure A.3 dAnkle and Percent Cured Surface Resin for 20 Trials (First Set of Experiments)

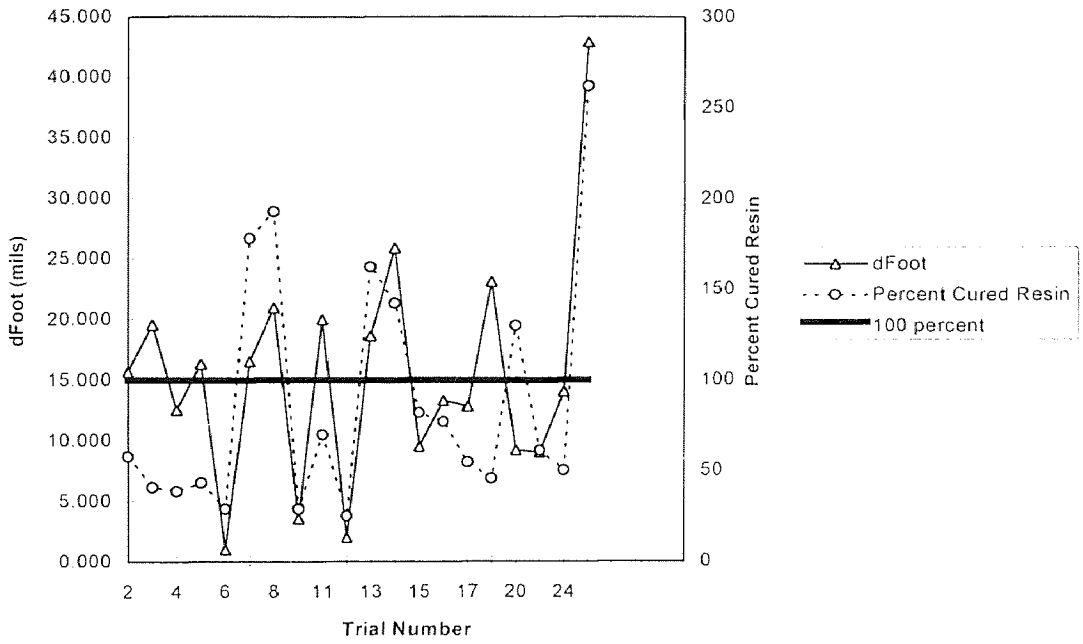

Figure A.4 dFoot and Percent Cured Surface Resin for 20 Trials (First Set of Experiments)

APPENDIX B

THE SECOND SET OF DATA

Included in this appendix is the L25 array parameter combinations used for the second set of data collection, the outputs as measured by CMM and the complete results gathered from the statistical analysis. The statistical analysis shows the effects of each factor level at each point of measurement. For example, in Table B.3 on page 57, are the effects of layer thickness, border overcure, hatch overcure, fill cure depth, fill spacing, and hatch spacing at point H-Top. The smallest value represents the optimal factor level, at this stage in the analysis. These points are highlighted. To obtain true optimal sets, more data needs to be collected based on focusing around the results gathered in this study. Tables B.4, B.5 and B.6 show the measurements taken at the Waist, Ankle, and Foot, respectively. For simplicity, Table B.7 shows all of the possible optimal parameters sets for each measurement location. These sets are comprised of the highlighted optimal factor levels. Lastly, in this appendix are the statistics used in determining the percent contribution of each build parameter for each measurement location. Table B.8, shows the percent contributions of layer thickness, border overcure hatch overcure, fill cure depth, fill spacing, and hatch spacing at location H-Top. Tables B.10, B.12, and B.14 show these same results for the Waist, Ankle, and Foot, respectively.

Table B.1 Orthogonal Array for the Second Set of Experiments

Trial	Layer Thickness	Border Overcure	Hatch Overcure	Fill Cure Depth (UF/DF) Up Facing/Down Facing	Fill Spacing	Hatch Spacing
1	0.006	0.007	-0.003	0.005/0.009	0.004	0.004
2	0.006	0.005	-0.004	0.003/0.007	0.003	0.002
3	0.006	0.009	-0.001	0.007/0.011	0.006	0.006
4	0.006	0.013	0.003	0.011/0.015	0.010	0.010
5	0.006	0.011	0.000	0.009/0.013	0.008	0.008
6	0.004	0.005	-0.001	0.005/0.009	0.010	0.008
7	0.004	0.009	0.003	0.003/0.007	0.008	0.004
8	0.004	0.013	0.000	0.007/0.011	0.004	0.002
9	0.004	0.011	-0.003	0.011/0.015	0.003	0.006
10	0.004	0.007	-0.004	0.009/0.013	0.006	0.010
11	0.008	0.009	0.000	0.005/0.009	0.003	0.010
12	0.008	0.013	-0.003	0.003/0.007	0.006	0.008
13	0.008	0.011	-0.004	0.007/0.011	0.010	0.004
14	0.008	0.007	-0.001	0.011/0.015	0.008	0.002
15	0.008	0.005	0.003	0.009/0.013	0.004	0.006
16	0.012	0.013	-0.004	0.005/0.009	0.008	0.006
17	0.012	0.011	-0.001	0.003/0.007	0.004	0.010
18	0.012	0.007	0.003	0.007/0.011	0.003	0.008
19	0.012	0.005	0.000	0.011/0.015	0.006	0.004
20	0.012	0.009	-0.003	0.009/0.013	0.010	0.002
21	0.010	0.011	0.003	0.005/0.009	0.006	0.002
22	0.010	0.007	0.000	0.003/0.007	0.010	0.006
23	0.010	0.005	-0.003	0.007/0.011	0.008	0.010
24	0.010	0.009	-0.004	0.011/0.015	0.004	0.008
25	0.010	0.013	-0.001	0.009/0.013	0.003	0.004

Table B.2 Output Data for the Second Set of Experiments

TRIAL	H-TOP	dH-TOP	B-TOP	dB-TOP	WAIST	dWAIST	ANKLE	dANKLE	FOOT	dFOOT
1	4.002	0.005	4.007	0.000	3.997	0.010	4.016	-0.009	4.020	-0.013
2	4.002	0.004	4.006	0.000	3.995	0.011	4.017	-0.011	4.020	-0.014
3	4.001	0.004	4.005	0.000	3.995	0.010	4.013	-0.008	4.016	-0.011
4	4.003	0.003	4.006	0.000	3.997	0.009	4.013	-0.007	4.016	-0.010
5	4.001	0.003	4.004	0.000	3.996	0.008	4.013	-0.009	4.015	-0.011
6	4.002	0.004	4.006	0.000	3.999	0.007	4.012	-0.006	4.014	-0.008
7	4.001	0.005	4.006	0.000	3.994	0.012	4.019	-0.013	4.023	-0.017
8	4.001	0.004	4.005	0.000	3.992	0.013	4.014	-0.009	4.018	-0.013
9	4.000	0.003	4.003	0.000	3.994	0.009	4.007	-0.004	4.009	-0.006
10	4.059	-0.010	4.049	0.000	4.042	0.007	4.023	0.026	4.028	0.021
11	3.994	0.009	4.003	0.000	3.991	0.012	4.016	-0.013	4.022	-0.019
12	3.990	0.008	3.998	0.000	3.993	0.005	4.007	-0.009	4.010	-0.012
13	3.998	0.005	4.003	0.000	3.991	0.012	4.015	-0.012	4.020	-0.017
14	3.986	0.013	3.999	0.000	3.975	0.024	4.030	-0.031	4.047	-0.048
15	3.992	0.008	4.000	0.000	3.979	0.021	4.032	-0.032	4.057	-0.057
16	3.990	0.008	3.998	0.000	3.981	0.017	4.011	-0.013	4.016	-0.018
17	3.986	0.010	3.996	0.000	3.981	0.015	4.012	-0.016	4.017	-0.021
18	3.984	0.013	3.997	0.000	3.970	0.027	4.038	-0.041	4.049	-0.052
19	3.982	0.013	3.995	0.000	3.970	0.025	4.036	-0.041	4.059	-0.064
20	3.983	0.013	3.996	0.000	3.972	0.024	4.040	-0.044	4.052	-0.056
21	3.992	0.012	4.004	0.000	3.987	0.017	4.030	-0.026	4.036	-0.032
22	3.993	0.006	3.999	0.000	3.983	0.016	4.020	-0.021	4.032	-0.033
23	3.985	0.017	4.002	0.000	3.996	0.006	4.011	-0.009	4.015	-0.013
24	3.993	0.010	4.003	0.000	3.996	0.007	4.012	-0.009	4.015	-0.012
25	3.986	0.009	3.995	0.000	3.977	0.018	4.016	-0.021	4.023	-0.028
SUM		0.179		0.000		0.342		-0.388		-0.564
average		0.0072		0		0.01368		-0.0155		-0.023

Table B.3 Effects of each Factor Level for dH-Top

*****	OPTIMUM

Overall mean value:
m = 0.00716

LAYER THICKNESS			
AT 0.006		$m_{0.006}$ =	0.0038
AT 0.004	*****	**m0.004 =**	**0.0012**
AT 0.008		$m_{0.008}$ =	0.0086
AT 0.012		$m_{0.012}$ =	0.0114
AT 0.010		$m_{0.010}$ =	0.0108
BORDER OVERCURE			
AT 0.007	*****	**m0.007 =**	**0.0054**
AT 0.005		$m_{0.005}$ =	0.0092
AT 0.009		$m_{0.009}$ =	0.0082
AT 0.013		$m_{0.013}$ =	0.0064
AT 0.011		$m_{0.011}$ =	0.0066
HATCH OVERCURE			
AT -0.003		$m_{-0.003}$ =	0.0092
AT -0.004	*****	**m-0.004 =**	**0.0034**
AT -0.001		$m_{-0.001}$ =	0.008
AT 0.003		$m_{0.003}$ =	0.0082
AT 0.000		$m_{0.000}$ =	0.007
FILL CURE DEPTH			
AT 0.005/0.009		$m_{0.005/0.009}$ =	0.0076
AT 0.003/0.007		$m_{0.003/0.007}$ =	0.0066
AT 0.007/0.011		$m_{0.007/0.011}$ =	0.0086
AT 0.011/0.015		$m_{0.011/0.015}$ =	0.0084
AT 0.009/0.013	*****	**m0.009/0.013 =**	**0.0046**
FILL SPACING			
AT 0.004		$m_{0.004}$ =	0.0074
AT 0.003		$m_{0.003}$ =	0.0076
AT 0.006	*****	**m0.006 =**	**0.0054**
AT 0.010		$m_{0.010}$ =	0.0062
AT 0.008		$m_{0.008}$ =	0.0092
HATCH SPACING			
AT 0.004		$m_{0.004}$ =	0.0074
AT 0.002		$m_{0.002}$ =	0.0092
AT 0.006	*****	**m0.006 =**	**0.0058**
AT 0.010	*****	**m0.010 =**	**0.0058**
AT 0.008		$m_{0.008}$ =	0.0076

Table B.4 Effects of each Factor Level for dWaist

	*****	OPTIMUM	

Overall mean value:
m = 0.01368

LAYER THICKNESS			
AT 0.006	*****	m0.006 =	0.0096
AT 0.004	*****	m0.004 =	0.0096
AT 0.008		$m_{0.008}$ =	0.0148
AT 0.012		$m_{0.012}$ =	0.0216
AT 0.010		$m_{0.010}$ =	0.0128
BORDER OVERCURE			
AT 0.007		$m_{0.007}$ =	0.0168
AT 0.005		$m_{0.005}$ =	0.014
AT 0.009		$m_{0.009}$ =	0.013
AT 0.013		$m_{0.013}$ =	0.0124
AT 0.011	*****	m0.011 =	0.0122
HATCH OVERCURE			
AT -0.003	*****	m-0.003 =	0.0108
AT -0.004	*****	m-0.004 =	0.0108
AT -0.001		$m_{-0.001}$ =	0.0148
AT 0.003		$m_{0.003}$ =	0.0172
AT 0.000		$m_{0.000}$ =	0.0148
FILL CURE DEPTH			
AT 0.005/0.009		$m_{0.005/0.009}$ =	0.0126
AT 0.003/0.007	*****	m0.003/0.007 =	0.0118
AT 0.007/0.011		$m_{0.007/0.011}$ =	0.0136
AT 0.011/0.015		$m_{0.011/0.015}$ =	0.0148
AT 0.009/0.013		$m_{0.009/0.013}$ =	0.0156
FILL SPACING			
AT 0.004		$m_{0.004}$ =	0.0132
AT 0.003		$m_{0.003}$ =	0.0154
AT 0.006	*****	m0.006 =	0.0128
AT 0.010		$m_{0.010}$ =	0.0136
AT 0.008		$m_{0.008}$ =	0.0134
HATCH SPACING			
AT 0.004		$m_{0.004}$ =	0.0154
AT 0.002		$m_{0.002}$ =	0.0178
AT 0.006		$m_{0.006}$ =	0.0146
AT 0.010	*****	m0.010 =	0.0098
AT 0.008		$m_{0.008}$ =	0.0108

Table B.5 Effects of each Factor Level for dAnkle

***** OPTIMUM

Overall mean value:
m = -0.01552

LAYER THICKNESS			
AT 0.006		$m_{0.006}$ =	-0.0088
AT 0.004	*****	**m0.004 =**	**-0.0012**
AT 0.008		$m_{0.008}$ =	-0.0194
AT 0.012		$m_{0.012}$ =	-0.031
AT 0.010		$m_{0.010}$ =	-0.0172
BORDER OVERCURE			
AT 0.007		$m_{0.007}$ =	-0.0152
AT 0.005		$m_{0.005}$ =	-0.0198
AT 0.009		$m_{0.009}$ =	-0.0174
AT 0.013	*****	**m0.013 =**	**-0.0118**
AT 0.011		$m_{0.011}$ =	-0.0134
HATCH OVERCURE			
AT -0.003		$m_{-0.003}$ =	-0.015
AT -0.004	*****	**m-0.004 =**	**-0.0038**
AT -0.001		$m_{-0.001}$ =	-0.0164
AT 0.003		$m_{0.003}$ =	-0.0238
AT 0.000		$m_{0.000}$ =	-0.0186
FILL CURE DEPTH			
AT 0.005/0.009	*****	**m0.005/0.009 =**	**-0.0134**
AT 0.003/0.007		$m_{0.003/0.007}$ =	-0.014
AT 0.007/0.011		$m_{0.007/0.011}$ =	-0.0158
AT 0.011/0.015		$m_{0.011/0.015}$ =	-0.0184
AT 0.009/0.013		$m_{0.009/0.013}$ =	-0.016
FILL SPACING			
AT 0.004		$m_{0.004}$ =	-0.015
AT 0.003		$m_{0.003}$ =	-0.018
AT 0.006	*****	**m0.006 =**	**-0.0116**
AT 0.010		$m_{0.010}$ =	-0.018
AT 0.008		$m_{0.008}$ =	-0.015
HATCH SPACING			
AT 0.004		$m_{0.004}$ =	-0.0192
AT 0.002		$m_{0.002}$ =	-0.0242
AT 0.006		$m_{0.006}$ =	-0.0156
AT 0.010	*****	**m0.010 =**	**-0.0038**
AT 0.008		$m_{0.008}$ =	-0.0148

Table B.6 Effects of each Factor Level for dFoot

***** OPTIMUM

Overall mean value:
m = -0.02256

LAYER THICKNESS			
AT 0.006		$m_{0.006}$ =	-0.012
AT 0.004	*****	**m0.004 =**	**-0.005**
AT 0.008		$m_{0.008}$ =	-0.031
AT 0.012		$m_{0.012}$ =	-0.042
AT 0.010		$m_{0.010}$ =	-0.024
BORDER OVERCURE			
AT 0.007		$m_{0.007}$ =	-0.025
AT 0.005		$m_{0.005}$ =	-0.031
AT 0.009		$m_{0.009}$ =	-0.023
AT 0.013	*****	**m0.013 =**	**-0.016**
AT 0.011		$m_{0.011}$ =	-0.017
HATCH OVERCURE			
AT -0.003		$m_{-0.003}$ =	-0.02
AT -0.004	*****	**m-0.004 =**	**-0.008**
AT -0.001		$m_{-0.001}$ =	-0.023
AT 0.003		$m_{0.003}$ =	-0.034
AT 0.000		$m_{0.000}$ =	-0.028
FILL CURE DEPTH			
AT 0.005/0.009	*****	**m0.005/0.009 =**	**-0.018**
AT 0.003/0.007		$m_{0.003/0.007}$ =	-0.019
AT 0.007/0.011		$m_{0.007/0.011}$ =	-0.021
AT 0.011/0.015		$m_{0.011/0.015}$ =	-0.028
AT 0.009/0.013		$m_{0.009/0.013}$ =	-0.026
FILL SPACING			
AT 0.004		$m_{0.004}$ =	-0.023
AT 0.003		$m_{0.003}$ =	-0.024
AT 0.006	*****	**m0.006 =**	**-0.02**
AT 0.010		$m_{0.010}$ =	-0.025
AT 0.008		$m_{0.008}$ =	-0.021
HATCH SPACING			
AT 0.004		$m_{0.004}$ =	-0.028
AT 0.002		$m_{0.002}$ =	-0.033
AT 0.006		$m_{0.006}$ =	-0.025
AT 0.010	*****	**m0.010 =**	**-0.008**
AT 0.008		$m_{0.008}$ =	-0.019

Table B.7 Optimum Parameter Sets

dH-Top

LT	0.004	0.004
BO	0.007	0.007
HO	-0.004	-0.004
FCD (UF/DF)	0.009/0.013	0.009/0.013
FS	0.006	0.006
HS	0.006	0.01

dWaist

LT	0.004	0.004	0.006	0.006
BO	0.011	0.011	0.011	0.011
HO	-0.003	-0.004	-0.003	-0.004
FCD (UF/DF)	0.003/0.007	0.003/0.007	0.003/0.007	0.003/0.007
FS	0.006	0.006	0.006	0.006
HS	0.01	0.01	0.01	0.01

dAnkle

LT	0.004
BO	0.013
HO	-0.004
FCD (UF/DF)	0.005/0.009
FS	0.006
HS	0.01

dFoot

LT	0.004
BO	0.013
HO	-0.004
FCD(UF/DF)	0.005/0.009
FS	0.006
HS	0.01

Table B.8 Sum of Squares and Percent Contributions of each Factor at dH-Top

dH-TOP

GRAND TOTAL SUM OF SQUARES
0.001965

SUM OF SQUARES DUE TO MEAN
0.001282

TOTAL SUM OF SQUARES
0.000683

TOTAL SUM OF SQUARES (CHECK)
0.000683

SS LAYER THICKNESS	PERCENT CONTRIBUTION
0.00040056	58.61624912

SS BORDER OVERCURE	PERCENT CONTRIBUTION
0.0000462	6.754858347

SS HATCH OVERCURE	PERCENT CONTRIBUTION
0.00010056	14.7155233

SS FILL CURE DEPTH	PERCENT CONTRIBUTION
0.0000534	7.808475767

SS FILL SPACING	PERCENT CONTRIBUTION
0.0000422	6.169515336

SS HATCH SPACING	PERCENT CONTRIBUTION
0.0000406	5.935378132

100
TOTAL
PERCENT

Table B.9 ANOVA Table for dH-Top

ANOVA TABLE

FACTOR	DEGREES OF FREEDOM	SUM OF SQUARES	MEAN SQUARE		F
LT	4	0.0004006	0.0001001		9.324022
BO	4	0.0000462	0.0000115		
HO	4	0.0001006	0.0000251		2.340782
FCD	4	0.0000534	0.0000133		1.242086
FS	4	0.0000422	0.0000105		
HS	4	0.0000406	0.0000101		
ERROR	0	0			
TOTAL	24	0.00068336			
(ERROR)	12	0.00012888	0.0000107		

Table B.10 Sum of Squares and Percent Contributions of each Factor at dWaist

dWAIST

GRAND TOTAL SUM OF SQUARES

0.005686

SUM OF SQUARES DUE TO MEAN

0.004679

TOTAL SUM OF SQUARES

0.001007

TOTAL SUM OF SQUARES (CHECK)

0.001007

SS LAYER THICKNESS	PERCENT CONTRIBUTION
0.00049024	48.66195505

SS BORDER OVERCURE	PERCENT CONTRIBUTION
0.0000706	7.01183197

SS HATCH OVERCURE	PERCENT CONTRIBUTION
0.00015744	15.62772969

SS FILL CURE DEPTH	PERCENT CONTRIBUTION
0.0000482	4.788374494

SS FILL SPACING	PERCENT CONTRIBUTION
0.0000202	2.009052648

SS HATCH SPACING	PERCENT CONTRIBUTION
0.0002206	21.90105614

100
TOTAL
PERCENT

Table B.11 ANOVA Table for dWaist

ANOVA TABLE

FACTOR	DEGREES OF FREEDOM	SUM OF SQUARES	MEAN SQUARE		F
LT	4	0.0004902	0.0001226		91.62047
BO	4	0.0000706	0.0000177		
HO	4	0.0001574	0.0000394		29.42381
FCD	4	0.0000482	0.0000121		
FS	4	0.0000202	0.0000051		
HS	4	0.0002206	0.0000552		41.23519
ERROR	0	0			
TOTAL	24	0.00100744			
(ERROR)	12	0.0001391	0.0000013		

Table B.12 Sum of Squares and Percent Contributions of each Factor at dAnkle

dANKLE

GRAND TOTAL SUM OF SQUARES

0.011196

SUM OF SQUARES DUE TO MEAN

0.006022

TOTAL SUM OF SQUARES

0.005174

TOTAL SUM OF SQUARES (CHECK)

0.005174

SS LAYER THICKNESS	PERCENT CONTRIBUTION
0.0025386	49.06305081

SS BORDER OVERCURE	PERCENT CONTRIBUTION
0.0002014	3.893132131

SS HATCH OVERCURE	PERCENT CONTRIBUTION
0.0010822	20.91592195

SS FILL CURE DEPTH	PERCENT CONTRIBUTION
0.0000770	1.488914314

SS FILL SPACING	PERCENT CONTRIBUTION
0.0001410	2.72581094

SS HATCH SPACING	PERCENT CONTRIBUTION
0.0011338	21.91316986

100
TOTAL
PERCENT

Table B.13 ANOVA Table for dAnkle

ANOVA TABLE

FACTOR	DEGREES OF FREEDOM	SUM OF SQUARES	MEAN SQUARE		F
LT	4	0.0025386	0.0006347		18.15389
BO	4	0.0002014	0.0000504		
HO	4	0.0010822	0.0002706		7.73913
FCD	4	0.0000770	0.0000193		
FS	4	0.0001410	0.0000353		
HS	4	0.0011338	0.0002835		8.108124
ERROR	0	0			
TOTAL	24	0.00517424			
(ERROR)	12	0.0004195	0.0000350		

Table B.14 Sum of Squares and Percent Contributions of each Factor at dFoot

dFOOT

GRAND TOTAL SUM OF SQUARES

0.021964

SUM OF SQUARES DUE TO MEAN

0.012724

TOTAL SUM OF SQUARES

0.00924

TOTAL SUM OF SQUARES (CHECK)

0.00924

SS LAYER THICKNESS	PERCENT CONTRIBUTION
0.00444896	48.14808402

SS BORDER OVERCURE	PERCENT CONTRIBUTION
0.0007394	8.001593046

SS HATCH OVERCURE	PERCENT CONTRIBUTION
0.00185216	20.04467455

SS FILL CURE DEPTH	PERCENT CONTRIBUTION
0.0003774	4.083911967

SS FILL SPACING	PERCENT CONTRIBUTION
0.0000854	0.923793527

SS HATCH SPACING	PERCENT CONTRIBUTION
0.0017370	18.79794289

100
TOTAL
PERCENT

Table B.15 ANOVA Table for dFoot

ANOVA TABLE

FACTOR	DEGREES OF FREEDOM	SUM OF SQUARES	MEAN SQUARE		F
LT	4	0.0044490	0.0011122		11.10315
BO	4	0.0007394	0.0001848		
HO	4	0.0018522	0.0004630		4.622388
FCD	4	0.0003774	0.0000943		
FS	4	0.0000854	0.0000213		
HS	4	0.0017370	0.0004342		4.334886
ERROR	0	0			
TOTAL	24	0.00924016			
(ERROR)	12	0.0012021	0.0001002		

APPENDIX C

TIME PREDICTION RESULTS

This appendix gives a similar statistical breakdown as discussed in appendix B, however it shows the data calculated to predict the build times of various H-4 test parts.

Table C.1 Calculated Time Estimates for each Trial

	SCAN TIME	TOTAL TIME	RECOAT TIME
1	0.121	11.115	10.993
2	0.081	11.075	10.993
3	0.187	11.181	10.993
4	0.422	11.415	10.993
5	0.282	11.275	10.993
6	0.064	11.057	10.993
7	0.119	11.112	10.993
8	0.274	11.268	10.993
9	0.205	11.198	10.993
10	0.096	11.089	10.993
11	0.270	11.264	10.993
12	0.590	11.583	10.993
13	0.402	11.395	10.993
14	0.205	11.198	10.993
15	0.121	11.115	10.993
16	1.349	12.343	10.993
17	0.894	11.887	10.993
18	0.405	11.398	10.993
19	0.292	11.285	10.993
20	0.604	11.598	10.993
21	0.593	11.586	10.993
22	0.267	11.261	10.993
23	0.187	11.181	10.993
24	0.422	11.415	10.993
25	0.908	11.902	10.993
SUM		284.194	
average		11.368	

Table C.2 Predicted Time Optimal Parameter Set

OPTIMUM PARAMETER SETS

TIME

LT	0.004
BO	0.005
HO	0.000
FCD (UF/DF)	0.007/0.011
FS	0.006
HS	0.002

Table C.3 Effects of each Factor Level for Time

*****	**OPTIMUM**			
		LAYER THICKNESS		
Overall		AT 0.006	$m_{0.006}$ =	11.212
Mean Value:		AT 0.004	***** **m0.004 =**	**11.145**
m = 11.368		AT 0.008	$m_{0.008}$ =	11.311
		AT 0.012	$m_{0.012}$ =	11.702
		AT 0.010	$m_{0.010}$ =	11.469
		BORDER OVERCURE		
		AT 0.007	$m_{0.007}$ =	11.212
		AT 0.005	****** **m0.005 =**	**11.142**
		AT 0.009	$m_{0.009}$ =	11.314
		AT 0.013	$m_{0.013}$ =	11.702
		AT 0.011	$m_{0.011}$ =	11.468
		HATCH OVERCURE		
		AT -0.003	$m_{-0.003}$ =	11.335
		AT -0.004	$m_{-0.004}$ =	11.463
		AT -0.001	$m_{-0.001}$ =	11.445
		AT 0.003	$m_{0.003}$ =	11.325
		AT 0.000	***** **$m_{0.000}$ =**	**11.270**
		FILL CURE DEPTH		
		AT 0.005/0.009	$m_{0.005/0.009}$ =	11.473
		AT 0.003/0.007	$m_{0.003/0.007}$ =	11.383
		AT 0.007/0.011	***** **$m_{0.007/0.011}$ =**	**11.284**
		AT 0.011/0.015	$m_{0.011/0.015}$ =	11.302
		AT 0.009/0.013	$m_{0.009/0.013}$ =	11.396
		FILL SPACING		
		AT 0.004	$m_{0.004}$ =	11.360
		AT 0.003	$m_{0.003}$ =	11.367
		AT 0.006	***** **m0.006 =**	**11.345**
		AT 0.010	$m_{0.010}$ =	11.345
		AT 0.008	$m_{0.008}$ =	11.422
		HATCH SPACING		
		AT 0.004	$m_{0.004}$ =	11.362
		AT 0.002	****** **m0.002 =**	**11.345**
		AT 0.006	$m_{0.006}$ =	11.419
		AT 0.010	$m_{0.010}$ =	11.367
		AT 0.008	$m_{0.008}$ =	11.346

Table C.4 Sum of Squares and Percent Contributions for each Factor for Time

TIME

GRAND TOTAL SUM OF SQUARES

3232.92558

SUM OF SQUARES DUE TO MEAN

3230.63856

TOTAL SUM OF SQUARES

2.28702541

TOTAL SUM OF SQUARES (CHECK)

2.28702541

SS LAYER THICKNESS	PERCENT CONTRIBUTION
0.995760744	43.53955749

SS BORDER OVERCURE	PERCENT CONTRIBUTION
0.99890	43.67681486

SS HATCH OVERCURE	PERCENT CONTRIBUTION
0.137327114	6.004616902

SS FILL CURE DEPTH	PERCENT CONTRIBUTION
0.116383	5.088833629

SS FILL SPACING	PERCENT CONTRIBUTION
0.020062	0.877225934

SS HATCH SPACING	PERCENT CONTRIBUTION
0.018592	0.81295119

100
TOTAL
PERCENT

Table C.5 ANOVA Table for Time

ANOVA TABLE

FACTOR	DEGREES OF FREEDOM	SUM OF SQUARES	MEAN SQUARE		F
LT	4	0.9957607	0.2489402		2.87915656
BO	4	0.9988999	0.2497250		
HO	4	0.1373271	0.0343318		0.39706954
FCD	4	0.1163829	0.0290957		0.3365112
FS	4	0.0200624	0.0050156		
HS	4	0.0185924	0.0046481		
ERROR	0	4.44089E-16			
TOTAL	24	2.287025411			
(ERROR)	12	1.037554635	0.0864629		

REFERENCES

Chen, Calvin C., Paul Sullivan. 1996. "Build Time Prediction and Time Related Issues for the Stereolithography Machine." *Proceedings of North American Stereolithography User Group Conference and Annual Meeting.* Tampa, Florida. March 12 - 16.

Flory, Paul J. 1953. *Principles of Polymer Chemistry.* Ithaca, New York: Cornell University Press.

Jacobs, Paul F. et al. 1992. *Rapid Prototyping and Manufacturing: Fundamentals of Stereolithography.* New York: McGraw-Hill

Jacobs, Paul F. et al. 1996. *Stereolithography and Other RP&M Technologies: from Rapid Prototyping to Rapid Tooling.* New York: ASME Press

Jacobs, Paul F. 1996. "Stereolithography Error Analysis." *Proceedings of North American Stereolithography User Group Conference and Annual Meeting.* Tampa, Florida. March 12 - 16.

Jayanthi, Suresh, Michael Keefe, Edward P. Gargiulo. 1994. "Studies in Stereolithography: Influence of Process Parameters on Curl Distortion in Photopolymer Models." *Proceedings of Solid Freeform Fabrication Symposium.* University of Texas. Austin, Texas. August 8 - 10.

Jayanthi, Suresh. 1995. "Studies in Stereolithography: Influence of Build Process Parameters on Curl Distortion." Master's Thesis, University of Delaware. Newark, Delaware.

Pang, Thomas H., Michelle D. Guertin, Hop D. Nguyen. 1995. "Accuracy of Stereolithography Parts: Mechanism and Modes of Distortion for a 'Letter-H' Diagnostic Part." *Proceedings of North American Stereolithography User Group Conference and Annual Meeting.* Tampa, Florida. March 12 - 16.

Pang, Thomas H.1994. "Stereolithography Epoxy Resins SL 5170 and SL 5180: Accuracy, Dimensional Stability, and Mechanical Properties." *Proceedings of Solid Freeform Fabrication Symposium.* University of Texas. Austin, Texas. August 8 - 10.

Phadke, Madhav S. 1989. *Quality Engineering Using Robust Design.* Englewood Cliffs, New Jersey: Prentice-Hall.